This is a preprint, the final version is subject to change, of the American Mineralogist (MSA)
Cite as Authors (Year) Title. American Mineralogist, in press.
(DOI will not work until issue is live.) DOI: http://dx.doi.org/10.2138/am.2013.4336

REVISION #3

Generalizations about monazite: Implications for geochronologic studies

Elizabeth J. Catlos

University of Texas at Austin, Jackson School of Geosciences, Dept. of Geological Sciences, 1 University Sta. C9000 EPS 1.130, Austin, TX 78712, USA

Abstract. With the advent of techniques that preclude mineral separation, ages from specific compositional domains in monazite [(Ce, La, Th)PO_4] have provided a wealth of information regarding the timing of the geologic evolution of numerous regions. However, confusion can arise when single grains show large differences in age that fail to correlate to chemistry or location within the monazite. Generalizations that lead to incorrect age interpretations include that monazite zoning in Y, Th, and/or the rare earth elements (REE) always identify (1) distinct tectonic events, (2) environment of crystallization, and (3) provenance of detrital grains. Increasing Th contents in monazite do not always reflect (1) increasing grade in metamorphic grains, (2) changes in silicate melt composition in igneous grains, (3) make the mineral more susceptible to alteration, nor (4) control the mineral's uptake of REE. Metamorphic monazites from Himalayan garnet-bearing rocks with co-existing allanite show no relationship between Th content and REE. Instead, chondrite-normalized REE patterns of the allanite mirror those of the monazite, indicating the variations are related to the reactant that formed the mineral. Generalizations about Pb behavior in monazite remain problematic. Incorporation of Pb into monazite has thus far been precluded by experimental studies, yet common Pb has been measured in many studies of natural monazite. A clear understanding about controls of monazite composition and the role of the chemical and/or pressure-temperature (P-T) environment of the rocks in which it forms is required to correctly interpret the meaning of the mineral's age(s).

Keywords. GEOCHRONOLOGY: ANALYSIS, CHEMICAL (MINERAL): ANALYSIS, CHEMICAL (ROCK): TRACE ELEMENTS AND REE: METAMORPHIC PETROLOGY

INTRODUCTION

Monazite (Ce, La, Th)PO_4 is often found in nature as a complexly zoned mineral (e.g., Zhu and O'Nions 1999a; Catlos et al. 2002; Foster et al. 2002; Pyle and Spear 2003; Gibson et al. 2004; Goncalves et al. 2005; Hinchey et al. 2007; Williams et al. 2007; Gasser et al. 2012). It typically contains large amount of radiogenic elements and can be dated using a variety of methods (isotope dilution, electron microprobe, ion microprobe; see reviews by Harrison et al. 2002 and Williams et al. 2007). Differences in the chemistry of specific zones in monazite are often attributed to differences in age and, in some cases, these regions can vary by many millions of years (e.g., Ayers et al. 1999; Gibson et al. 2004; Mahan et al. 2006; Santosh et al. 2006). However, some grains have unexpected internal age relationships. For example, some monazite grains show older ages near apparent rims and younger ages near the core (Fig. 1 in Ayers et al. 1999; Fig. 7A in Gibson et al. 2004; Fig. 9 in Catlos et al. 2008; multiple grains in Triantafyllidis et al. 2010). Some grains have clear correlations between Y content and age (e.g., Shaw et al. 2001; Gibson et al. 2004; Krenn et al. 2009; Martins et al. 2009), yet in others no such obvious relationship exists (e.g., Hokada and Motoyoshi 2006; Hinchey et al. 2007; Martin et al. 2007; Triantafyllidis et al. 2010; Reno et al. 2012). Compositional differences among zones in monazite, although providing a qualitative impression of the evolution of the crystal through time, may not always record a clear age progression (e.g., Spear and Pyle 2010) nor reflect a simple evolution of a given system (e.g., Wark and Miller 1993; Kelly et al. 2012). Chemical variations can create misleading expectations regarding its number of growth stages, and thus the

number of temporally distinct tectonic episodes the mineral, rock, and/or region experienced and recorded.

In addition, monazite composition, zoning, and even its shape have been suggested to identify its origin in specific rock types (e.g., Overstreet 1967; Mohr 1984; Schandl and Gorton 2004; Förster 1998; Broska et al. 2000; Townsend et al. 2000; Dawood and El-Naby 2007; Dill et al. 2012). The distribution of specific elements in monazite, like Y, Th, and rare earth elements (REE) as a tool to discriminate for provenance would be beneficial if they could decipher the source of detrital grains (e.g., Iizuka et al. 2010). Here, correlations between monazite chemistry, zoning, morphology and provenance are explored to test some of these generalizations and examine their use for environmental discrimination.

MONAZITE ZONING AND STRUCTURE

The monazite structure consists of distorted PO_4 tetrahedra (Huminicki and Hawthorne 2002). Monazite is considered a "large cation" phosphate mineral with a space group of $P2_1/n$ ($Z=4$) (Mooney 1948; Beall et al. 1981; Deer et al. 1992; Ni et al. 1995; Huminicki and Hawthorne 2002; Clavier et al. 2011). The mineral preferentially incorporates light rare earth elements ($LREE^{3+}$) (Amli 1975; Ilupin et al. l971), which are coordinated with nine O-atoms (Ni et al. 1995; Huminicki and Hawthorne 2002). The nine-fold coordination polyhedra share edges to form chains in the b-direction of the mineral and stack in the a-direction (Fig. 1) (e.g., Ni et al. 1995; Huminicki and Hawthorne 2002; Clavier et al. 2011). REE-P distances vary with atomic number and decrease with decreasing REE^{3+} radius (Ni et al. 1995). Because of this, the size of the REE^{3+} cation influences the probability of uptake in specific sites, and these sites discriminate between REE^{3+} depending on growth surface (Cressey et al. 1999; Popova and Churin 2010). The ability of its 9-fold coordination polyhedra to distort and accommodate a

large variety of cations (e.g., Th^{4+}, Y^{3+}, U^{4+}, Pb^{2+}) allows the structure to exhibit chemical flexibility and is likely the explanation for why the monazite is stable over a range of pressure-temperature (P-T) conditions, is durable, and resistant to radiation damage (Dubrail et al. 2009; Huang et al. 2010; Clavier et al. 2011; Seydoux-Guillaume et al. 2002a).

Sector-zoned minerals are indicative of a metastable state (e.g., Dowty 1976) and are unavoidable in crystals, like monazite, that exhibit selective enrichment (e.g., Cressey et al. 1999) and slow lattice diffusion (e.g., Watson and Liang 1995; Teufel and Heinrich 1997; Seydoux-Guillaume et al. 2002a,b; Cherniak et al. 2004; Harlov et al. 2007). Two major mechanisms contribute to sector zoning: (1) selective adsorption on the crystal surface or (2) different attachment kinetics on different facets (Shtukenberg et al. 2009). Sector-zoned monazite has been produced during monazite/melt partitioning experiments (Stepanov et al. 2012). The complex interplay between compositionally distinct sectors in different crystals of monazite can lead to some of the types of zoning patterns observed in nature as multiple crystals develop into an apparent single grain, similar as to what has been observed in tourmaline and epidote (e.g., Choo 2002; 2003) and could be related to what has been described in monazite as "spotted zoning" (e.g., Fig. 15A in Aleinikoff et al. 2000).

Secondary processes, like interactions with fluids and recrystallization, can alter monazite's primary zoning and lead to a host of variations in the appearance of the mineral in backscattered electron (BSE) images and X-ray element maps (e.g., Harlov and Hetherington 2010; Harlov et al. 2011; Kelly et al. 2012). Although a long residence time at high temperature can alter sector zoning (e.g., Loomis 1983), this is unlikely to operate in monazite as diffusion of large cations is slow (Watson and Liang 1995; Teufel and Heinrich 1997; Seydoux-Guillaume et al. 2002a.b; Cherniak et al. 2004; Harlov et al. 2007; Cherniak and Pyle 2008; Cherniak 2010;

Chen et al. 2012). Primary sector zoning of monazite is rarely reported (Cressey et al. 1999; Williams et al. 2007; Iizuka et al. 2010; Popova and Churin 2010) and is sometimes seen in combination with other types of zoning (Hawkings and Bowing 1997; Crowley and Ghent 1999; Crowley et al. 2008). Some monazite grains described as "sector zoned" show differences in BSE more consistent with secondary zoning, such as curved rims and embayed grain interiors (e.g., Fig. 7B in Wan et al. 2005). Some single monazite grains display combinations of zoning types in BSE (e.g., patchy and oscillatory, Catlos et al. 2002, Aleinikoff et al. 2000; patchy and irregular, Rubatto et al. 2006).

Table 1 attempts to describe and define the types of monazite zoning with examples from the literature. These examples suggest that it can be difficult to distinguish between "oscillatory" and "patchy" or "irregular" zoning (e.g., Fig. 15B in Aleinikoff et al. 2000; Fig. 3A in Sindern et al. 2012). The mineral's appearance in BSE is important in evaluating the role of secondary reactions that could affect its age. In an analysis of 324 detrital monazite grains, Triantafyllidis et al. (2010) suggests monazite zoning type can be divided into two categories: (1) simple, with a core surrounded by a simple rim, and (2) more complex, where a core of variable shape is enveloped by two or more circular rims that may be discontinuous. Most grains with BSE images reported in the literature fall in the "more complex" category, with concentric, patchy, and intergrowth-like zoning (Table 1, Ayers et al. 1999; Zhu and O'Nions 1999a). In BSE images, concentric zoning is reported to be the most common (Ayers et al. 1999; Zhu and O'Nions 1999a; Vavra and Schaltegger 1999; Swain et al. 2005; Williams et al. 2007; Bruguier et al. 2009), although this is disputed in Faure et al. (2008). Unzoned (examples in Amli 1975; Pe-pier and McKay 2006; Chen et al. 2012) and oscillatory zoned (Hawkings and Bowing 1997; Crowley et al. 2008; Kohn and Vervoot 2008) grains are more rare.

This is a preprint, the final version is subject to change, of the American Mineralogist (MSA)
Cite as Authors (Year) Title. American Mineralogist, in press.
(DOI will not work until issue is live.) DOI: http://dx.doi.org/10.2138/am.2013.4336

Although some attribute BSE zoning primarily to differences in Th content (Swain et al. 2005), linking the mineral's elemental contents to differences in contrast in BSE images can be challenging (e.g., Fig. 4 in Williams et al. 2007). Quantitative chemical analysis or qualitative X-ray element mapping is required to understand which elements cause differences in brightness in BSE. Although Th is likely a major factor because of its large atomic number, different zoning types can exist within single grains, and the degree of contrast can be a result of multiple elements. For example, monazite grains have been reported showing oscillatory zoning in one element and normal zoning in others (e.g., Th and Y, Pe-pier and McKay 2006). Some grains with patchy zoning even show differences in the location of specific compositional domains (compare Th, Y, and Ce zoning in Kelly et al. 2012). Monazite can also recrystallize along microcracks, modifying compositions, and resulting in brightness differences (e.g., Crowley et al. 2008). Some grains show obvious internal recrystallization textures along what could have been healed microcracks; interestingly, ages from these recrystallization zones are similar to those from regions on the intact grain (e.g., Fig. 2 in Ayers et al. 2006; Fig. 2A in Shaw et al. 2001).

ROLE OF Th IN MONAZITE

Monazite is typically seen in nature as a Th-rich (as opposed to a U-rich) mineral (e.g., Overstreet 1967; Gramacciolii and Segalstad 1978; Deer et al. 1992). Normal zoning of monazite is defined as low Th cores and high Th rims (Zhu and O'Nions 1999a; Majka et al. 2012), although the terms "normal" and "reverse" to describe monazite appearance is uncommon. Monazite grains that grew along a prograde path show high Th cores and low Th rims (Kohn and Malloy 2004).

Thorium is commonly thought to enter the monazite structure with a 4+ oxidation state (Kelly et al. 1981; Hazen et al. 2009) via a coupled substitution with Si ($Th^{4+} + Si^{4+} \rightarrow REE^{3+} + P^{5+}$ e.g., monazite-huttonite join; Della Ventura et al. 1996), with Ca ($Th^{4+} + Ca^{2+} \rightarrow 2REE^{3+}$, monazite-brabanite join) (Starynkevitch 1922; Burt 1989; Förster 1998; Förster and Harlov 1999), and/or by other substitutions (see Table 2). Monazite/melt experiments conducted at 10-50 kbar and 750-1200°C show that partition coefficients for Th are 30% higher than those for the LREE (Stepanov et al. 2012). The pure huttonite substitution can be used to explain the presence of ThO_2 up to 27 wt% and REE_2O_3 to at least 20 wt%, at which divalent cations, F, and/or OH may be incorporated to maintain charge balance (Kucha 1980; Clavier et al. 2011). In synthetic monazite, Th may also enter the structure accompanied by a vacancy via $3Th^{4+}$ + vacancy→ $4REE^{3+}$, which appears to be restricted to ~17.68 wt% ThO_2 (Podor 1994; Clavier et al. 2011). Thorium may also be accompanied by a divalent cation: $REE^{3+}PO_4 + xM^{2+} + xTh^{4+} \rightarrow (REE^{3+}_{(1-2x)}M^{2+}_xTh^{4+}_x)PO_4 + 2xREE^{3+}$, where M^{2+} can be Ca^{2+}, Cd^{2+}, Sr^{2+}, Pb^{2+}, and Ba^{2+} (Quarton et al. 1984; Clavier et al. 2011).

Thorium contents have been suggested to increase with increasing metamorphic grade, with igneous monazite grains typically having the higher amounts (Overstreet 1967; Mohr 1984). However, Zhu and Onions (1999b) did not find this correlation. Carbonatites commonly contain monazite with low Th contents (e.g., Wall and Mariano 1996; Cressey et al. 1999; Pilipiuk et al. 2001; Catlos et al. 2008) as do authigenic monazite (Cabella et al. 2001; Čopjaková et al. 2011). ThO_2 content has been suggested as a means to distinguish hydrothermal (0-1 wt% ThO_2) from igneous monazite (3 to >5 wt% ThO_2; see Schandl and Gorton 2004) and many hydrothermal ore deposits also contain monazite with low Th (<2 wt% ThO_2, e.g., Bearss and Pitman 1996; Zhu and Onions 1999b; Pršek et al. 2010; Bonyadi et al. 2011; Sheard et al. 2012). Low Th ("Th-

160 free", ~0.2 ppm Th) grains have been found in hydrothermal tin vein deposits (Kempe et al.
161 2008). However, exceptions to this rule exist as hydrothermal monazite with 1.33 to 4.08 wt %
162 ThO_2 has been observed (Janots et al. 2012).

163 Monazite Th content in igneous rocks appears independent of that of the silicate melt
164 (Förster 1998) and Th-rich patches and/or variable compositions in monazite have been shown to
165 reflect fluid-induced alteration (e.g., Crowley et al. 2008; Harlov and Hetherington 2010; Kelly
166 et al. 2012; Janots et al. 2012). Thermometers involving monazite also rely on REE content
167 rather than Th (e.g., Gd, Gratz and Heinrich 1998; Y, Dy, and Gd, Pyle et al. 2001). Monazite
168 that has experienced dissolution and reprecipitation can show increases in Th at the rims (e.g.,
169 Watt 1995; Harlov and Hetherington 2010) and grains with mottled overgrowths that likely
170 interacted or grew via a fluid phase have high Th mid-rim contents (e.g., Rasmussen et al. 2007;
171 Rasmussen and Muhling 2007; 2009). Thorium may also be depleted in grains that have
172 experienced metasomatism (e.g., Schandl and Gorton 2004), but this depends largely on fluid
173 composition (Harlov et al. 2011; Janots et al. 2012).

174 Thorium-rich monazite has been suggested to be more susceptible to alteration than Th-
175 poor accessory minerals (Berger et al. 2008), although monazite is quite durable and is often
176 found as a detrital mineral (e.g., Pe-piper and McKay 2006; Triantafyllidis et al. 2010; Hietpas et
177 al. 2011). Experiments with monazite dissolution suggest that its Th-rich surfaces may dissolve
178 slower than those that are Th-poor (Oelkers and Poitrasson 2002). Monazite solubility has also
179 been shown to increase with increasing pressure with Th remaining relatively constant over the
180 range of experimental conditions (10-50 kbar and 750-1200°C, Stepanov et al. 2012). Monazite
181 is rarely found in nature in a metamict form; this may be due to the asymmetry of its structure
182 (e.g., Black et al. 1984; Clavier et al. 2011) and its ability to recover from radiation damage at

low temperature (e.g., Boatner and Sales 1988; Meldrum et al. 1998). The long half-life of ^{232}Th also contributes to the stability of monazite because the mineral, although containing large amounts of this radiogenic isotope, will not be subjected to the degree of radiation damage, Pb production, and auto-oxidation that are experienced by U-bearing minerals (Hazen et al. 2009). Ancient monazite (~2-3 Ga) with high ThO_2 contents (14.1-16.2 wt. %) have been found to be "not badly damaged" (Black et al. 1984). Monazite grains with high ThO_2 (up to 14.52 wt%) subjected to intense hydrothermal alteration were found to be the "most stable" when compared to zircon, fluorite, bastnasite, thorite, and xenotime (Breiter et al. 2009). Consistent with this observation, hydrothermally treated monazite grains of different size fractions have been shown to exhibit only minor dissolution features confined to the grain surfaces (Teufel and Heinrich 1997). However, Poitrasson et al. (2000) found that monazite can undergo changes at low temperature (260 to 340°C) when exposed to saline fluids.

Andrehs and Heinrich (1998) suggest that the incorporation of smaller cations of UO_2 + ThO_2 at levels >4 mol% saturate the monazite structure and suppress incorporation of $HREE^{3+}$. Table 3 lists the size of these cations in 9-fold coordination, which appear largely similar (Shannon 1976). Note that it can be difficult to measure the HREE contents in monazite due to low concentrations of these elements in the mineral, and many compositional analyses reported in the literature omit these analyses. In-line with the expected trend, monazite grains from granulite facies rocks with unusually high $HREE_2O_3$ +Y_2O_3 (12.5-25 wt%) show a systematic decrease in Er_2O_3 +Yb_2O_3 contents with increasing UO_2+ThO_2 (Fig. 2A; Krenn and Finger 2010). However, monazite grains from A-type granites (Xie et al. 2006) do not follow this trend (Fig. 2A). Instead, these grains remain constant in Er_2O_3 +Yb_2O_3 but exponentially decrease in LREE with increasing UO_2+ThO_2 (Fig. 2B), indicating that environment plays a role. In

206 metamorphic rocks, monazite grains that form after garnet breakdown contain higher amounts of
207 Y and HREE, a feature unrelated to their Th content (Zhu and Onions 1999b).

208 Because the size of the Th^{4+} ion is similar to Ce^{3+} (Table 3) (e.g., Demartin et al. 1991a),
209 expectations exist that monazite LREE contents are controlled by Th (Brouand and Cuney 1990;
210 Förster 1998). Chondrite-normalized REE patterns of monazite have been suggested to be
211 dependent on Th (Förster 1998; Stepanov et al. 2012). For example, a high-Th (~42 wt%) grain
212 termed "huttonitic monazite-Ce" from peraluminous granites has a steep chondrite-normalized
213 REE pattern, whereas those from low-Th (<1 wt%) grains are flat (Förster 1998). Figure 3A
214 shows that monazite from granulite facies rocks that contain $UO_2 + ThO_2 > 4$ wt% have, in
215 general, depleted HREE and enriched MREE compared to those with <4 wt% $UO_2 + ThO_2$
216 (Krenn and Finger 2010). However, monazite from A-type granites with $UO_2 + ThO_2 < 1$ wt%
217 show enriched LREE contents and overlap in their MREE and HREE compositions compared to
218 grains that range from 8.4 to 25.7 wt% $UO_2 + ThO_2$ (Fig 3B). Steepness in the REE patterns
219 appears unaffected by UO_2 and ThO_2 content. Further exploration of this trend using many high-
220 quality compositional analyses of detrital monazite grains reported by Triantafyllidis et al.
221 (2010) show monazite with $UO_2 + ThO_2$ of 8-17 wt% in general showing steeper LREE
222 chondrite-normalized patterns than those with low $UO_2 + ThO_2$ (<1 wt%) (Fig. 3C and D).
223 However, overlaps exist in the chondrite-normalized patterns between the high and low UO_2 +
224 ThO_2 monazite grains from these studies. The high $UO_2 + ThO_2$ monazite grains do appear to
225 have a more restricted range in LREE compositions. Triantafyllidis et al. (2010) filter their REE
226 patterns into 6 distinct trends in an attempt to link them to provenance.

227 Figure 4 shows chondrite-normalized REE patterns of metamorphic (Himalayan)
228 monazite with varying Th contents (from 0.29 to 15.8 wt%, see supplementary data). These

grains were collected from four garnet- and allanite-bearing assemblages of the Lesser Himalayan Formations (see Catlos et al. 2001 for sample locations and mineral assemblages) and analyzed using an electron microprobe following methods outlined in Catlos et al. (2002). These monazite grains do not show significant changes in REE patterns depending on $ThO_2 + UO_2$ content. Instead, variations appear related to allanite, the reactant that formed the mineral since the REE patterns of co-existing allanite grains in these rocks mirror those of the monazite. Although the monazite contains overall higher REE than co-existing allanite, they show no fractionation in their compositions, consistent with observations that REE can be largely immobile during metamorphism (e.g., Exley 1980; Bernard-Griffiths et al. 1985).

In addition, the chondrite normalized REE patterns of Himalayan monazite and allanite grains do not reflect the composition of the whole rock. Figure 5A shows the whole rock REE patterns from samples shown in Figure 4 and those from the same unit of the Lesser Himalayan formation that contain either monazite + allanite or allanite only (see Catlos 2000 for compositions). The whole-rock chondrite-normalized REE patterns differ from those of the monazite or co-existing allanite in that they show no Sm anomalies. The results support the observation that monazite composition in these rocks is dependent on the REE contents of the allanite, rather than the whole rock itself. This is consistent with the analysis of monazite and co-existing accessory minerals in metamorphic rocks elsewhere (Pan 1997; Upadhyay and Pruseth 2012). No relationship exists between the presence of these accessory minerals and (1) REE patterns nor (2) the Ca or Al contents of the whole rock (Fig. 5B, Wing et al. 2003).

Pb BEHAVIOR IN MONAZITE

A common assumptions about the presence of Pb in monazite is that radiogenic Pb is stable in natural monazite (e.g., Suzuki et al. 1994; Podor and Cuney 1997; Dubrail et al. 2009)

and that the mineral excludes common Pb during crystallization (e.g., Corfu 1988; Seydoux-Guillaume et al. 2002b). This assumption forms the basis for electron microprobe dating of monazite, as the method measures the total Pb, rather than each of the separate Pb isotopes in the mineral (e.g., Suzuki et al. 1994; Montel et al. 1996). The validity of this assumption has been tested by Williams et al. (2012) via experimental fluid-mediated alteration of monazite grains which resulted in complete "resetting" of monazite age and exclusion of Pb from the altered domains. Geochronologic methods that measure Pb isotopes in monazite, however, report common Pb (e.g., Tilton and Nicolaysen 1957; Parrish 1990; Boggs et al. 2002; Catlos and Cemen 2005; Hoisch et al. 2008; Kempe et al. 2008; Kohn and Vervoot 2008; Krenn et al. 2008a,b; Morelli et al. 2010; Aleinikoff et al. 2012; Janots et al. 2012; Seydoux-Guillaume et al. 2012). Higher amounts of common Pb are often found in monazite that forms in Pb-rich environments, like ore deposits (e.g., Lobato et al. 2007; Kempe et al. 2008; Krenn et al. 2008a; Krenn et al. 2011; Li et al. 2011). The monazite grain with the highest common Pb content ever reported is likely a hydrothermally-generated monazite grain from the Llallagua tin ore deposit in Bolivia, which has 99.9% common ^{206}Pb (Kempe et al. 2008).

Although some experimental studies have shown that common Pb is difficult to impossible to incorporate into the mineral structure (e.g., Corfu 1988; Seydoux-Guillaume et al. 2002b; Williams et al. 2012), fluids have been speculated as a mechanism to increase the common Pb contents of the mineral via dissolution-reprecipitation reactions (e.g., Janots et al. 2012). However, experiments with natural monazite by other workers show that it is also possible to increase common Pb contamination under conditions where hydrothermal alteration is not a factor (Teufel and Heinrich 1997). Common Pb measured during the analysis of monazite is also speculated to originate at grain boundaries or within microfractures rather than

intrinsic to the grain itself (e.g., Hoisch et al. 2008; Janots et al. 2012; Seydoux-Guillaume et al. 2012).

Dates generated from the same region in monazite grains using both the electron microprobe and high-resolution secondary ion mass spectrometery have been found to differ slightly, a difference ascribed to the lack of measurement of common Pb with the electron microprobe (Sano et al. 2006). The difference appears to become more pronounced as the dates get older (see Sano et al. 2006 and compare the Triassic and Proterozoic results). Radiogenic ^{208}Pb* contents of monazite grains from Turkish metagranites (Catlos et al. 2010) measured using in situ (in thin section) using an ion microprobe average 68.9±3.4%, whereas grains from metapelites average 80.3±1.4% (Catlos and Cemen 2005) (Figure 6). Monazite grains dated from the same granite body using isotopic dilution methods are ~97% ^{208}Pb* (Glodny and Hetzel 2007). The ion microprobe method sputters ions to depths of < 1μm of the grain surface during a typical analysis, so common Pb contents may be higher if the element is hosted in fractures, along grain boundaries, and/or as surface contamination, rather than in the grains themselves (e.g., Hoisch et al. 2008; Janots et al. 2012). In their ion microprobe study of monazite, Santo et al. (2006) state the source common Pb in their dated grains "is not easy to assess."

To understand where Pb could reside in the monazite structure requires some knowledge of its oxidation state. However, disagreements exist regarding the oxidation state of radiogenic Pb in monazite. For example, Petrik and Konecny (2009) suggest both Pb^{2+} and Pb^{4+} can be accommodated in the monazite structure and that radiogenic Pb may change oxidation state in the mineral (see Hazen et al. 2009 for a description of the process in zircon). Frei et al. (1997) suggests that during radiogenic decay, all Pb exists in the 4+ oxidation state as valence electrons are stripped during the recoil process. Alternatively, Pb^{4+} may not exist in nature because it is a

298 powerful oxidant (Podor and Cuney 1997). X-ray Absorption Near Edge Structure (XANES)
299 studies show Pb^{2+} is present and stable in natural monazite and likely substitutes for La^{3+}
300 (Dubrail et al. 2009). These cations are similar in their ionic radii (Table 3). These studies also
301 suggest that natural monazite grains will reject Pb due to its larger size when it crystallizes, and
302 thus most of the element present in the mineral will be due to radiogenic decay of Th and U
303 (Dubrail et al. 2009). Podor and Cuney (1997) suggest Pb^{2+} can substitute for Ca^{2+} in its original
304 site and for REE if charge is compensated by U^{4+} or Th^{4+}. Lead in the 2+ and 4+ oxidation states
305 differ significantly (1.35 vs. 0.94Å) (Table 3). The difference between the ionic radius of Th^{4+}
306 and Pb^{2+} is almost 20% (Table 3), suggesting the site increases in size to accommodate the
307 daughter product after radiogenic decay if the Pb^{2+} cation remains in the same site as the parent.
308 A second assumption regarding Pb behavior in monazite is that diffusion of the cation in
309 monazite is negligible, even at high-grade conditions (e.g., Cherniak et al. 2004; Gardes et al.
310 2006). However, depth profiling studies directly measuring the distribution of Pb in the
311 outermost rims of unpolished monazite show behavior consistent with Pb diffusion in rocks that
312 experienced peak T of ~500ºC (~20 km depth assuming geothermal gradient of 25ºC/km, Grove
313 and Harrison 1999) and ~900±25°C (McFarlane and Harrison 2006). The discrepancy between
314 studies of monazite that suggest the mineral can lose Pb via diffusion at moderate crustal
315 conditions (e.g., Suzuki et al. 1994; Smith and Giletti 1997) and those that suggest it is highly
316 retentive even at high (>800ºC) temperatures (e.g., Cherniak et al. 2004; Gardes et al. 2006) may
317 be attributed to differences in (1) trace element variations and potential for vacancies in natural
318 versus synthetic monazites, (2) experimental conditions in the diffusive Pb loss studies, and/or
319 (3) potential for diffusion along different crystal faces in the mineral (e.g., Gardes et al. 2006;
320 McFarlane and Harrison 2006).

THE Y PROBLEM

Correlations exist in some monazite grains between Y content and age (e.g., Dahl et al. 2005; Mahan et al. 2006; Chatterjee et al. 2010), but the absence of this observation in others (e.g., Hokada and Motoyoshi 2006; Hinchey et al. 2007; Martin et al. 2007; Triantafyllidis et al. 2010; Reno et al. 2012) makes the generalization that significant fluctuations Y monazite always relate to changes in large-scale tectonic conditions suspect. The presence of Y in high amounts in monazite is unusual. The element is smaller and heavier than LREE (Table 3) and would is more typically hosted in xenotime (e.g., Felsche 1976; Ni et al. 1995; Andrehs and Heinrich 1998; Huminicki and Hawthorne 2002; Krenn and Finger 2010). The presence of Y is thought to contract the monazite structure (e.g., Bowie and Horne 1953; Ni et al. 1995; Petrik and Konecny 2009). Although the radius of Y^{3+} and Gd^{3+} are similar (Table 3), fractionation between the two in the monazite structure is not solely governed by ionic radii (e.g., Demartin et al.1991a,b) and these elements do not behave in a similar fashion.

Monazite and xenotime have a well-known miscibility gap (e.g., Gratz and Heinrich 1997; Mogilevsky 2007) and higher amounts of Y in monazite in metamorphic rocks may be related to increasing grade (e.g., Heinrich et al. 1997; Zhou et al. 2008; Krenn and Finger 2010). In synthetic monazite, increasing temperature and pressure leads to an increase in the solid state solubility of YPO_4 in $LREEPO_4$ compounds (Van Emden et al. 1997a; Andrehs and Heinrich 1998; Gratz and Heinrich 1998; Seydoux-Guillaume et al. 2002b; Mogilevsky 2007; Maslennikova et al. 2010; Clavier et al. 2011). Thus, it seems reasonable to expect that high Y monazite likely formed at higher-grade conditions (e.g., Krenn and Finger 2010), although some high Y zones in monazite in metamorphic rocks can also be related to increases in Y in the

crystallization environment due to the breakdown of garnet and/or other accessory minerals (e.g., Mahan et al. 2006; Zhu and Onions 1999b; Spear and Pyle 2010).

The source of Y in monazite in metamorphosed pelites is speculated to be reactions involving garnet, and high-Y rings (annuli) in garnet appear at conditions linked to the appearance of the mineral in the rock (e.g., Kohn and Malloy 2004; Catlos et al. 2001). Alternatively, the presence of Y in garnet has been speculated to be due to the breakdown of accessory minerals, like xenotime or allanite (Yang and Rivers 2002; Yang and Pattison 2006; Giere et al. 2011; Marsh et al. 2012). High-Y garnets typically contain only ~1% Y_2O_3 (Zeh 2006; Honig et al. 2010). In low-grade metamorphic assemblages, allanite or xenotime are the dominant sinks for Y (e.g., Regis et al. 2012) and are also major contributors of Y to monazite during metamorphism (Spear and Pyle 2010). Petrogenetic modeling of low Ca pelites suggests monazite mode and composition are controlled by the presence of xenotime in metamorphic rocks, and when this mineral is absent, by the growth or consumption of garnet (Spear and Pyle 2010).

The roles of reactant availability, open system behavior, and the preference of the mineral structure in determining the composition of monazite is exemplified by its Y content. Although Y zoning in monazite provides a map for geochronologists in choosing specific zones in the mineral to date, the lack of correlation between age and Y contents in some monazite (e.g., Martins et al. 2009; Triantafyllidis et al. 2010) suggests that no expectations should exist that variations in Y content directly correlate to temporal or tectonic changes. A complexly zoned grain may form at a single time or within the ability of an instrument to resolve the time frame over which it grew. In metamorphic rocks, the breakdown of different minerals that provide its

365 constituents (i.e., allanite, xenotime, garnet) at different points along its path though P-T space
366 contributes to its compositional differences (e.g., Spear and Pyle 2010).

367 **MONAZITE COMPOSITION, SHAPE, AND PROVENANCE**

368 Monazite zoning has been speculated to be a useful indicator of environment as the
369 mineral can preserve complex internal zonation patterns at high metamorphic grade (e.g.,
370 Williams et al. 2007). Sector- and oscillatory-zoned monazite is thought to be typical of igneous
371 rocks and patchy zoning characteristic of metamorphic assemblages (Broska et al. 2000;
372 Townsend et al. 2000; Dawood and El-Naby 2007). This assumption would be useful in
373 deciphering the provenance of detrital monazite. However, oscillatory zoning has been found in
374 amphibolite-granulite grade monazite (e.g., Aleinikoff et al. 2006) and a monazite that
375 experienced amphibolite facies shows both sector zoning and oscillatory zoning (Crowley and
376 Ghent 1999). Monazite with patchy zoning has been found in granitic assemblages that
377 experienced metamorphism and metasomatism during exhumation (e.g., Catlos et al. 2010).

378 Monazite composition and zoning will be influenced by reactants available in its
379 chemical environment, the P-T path that the rock follows (e.g., Wark and Miller 1993; Spear and
380 Pyle 2010), the preference of the crystal to accept specific elements during growth (e.g., Cressey
381 et al. 1999), and interaction with fluids (e.g., Harlov and Hetherington 2010; Harlov et al. 2011).
382 The assumption that monazite composition in plutonic rocks will simply reflect the fractional
383 crystallization of the melt has been shown to be complicated by the potential for magma mixing,
384 metasomatism, and alteration (Wark and Miller 1993; Catlos et al. 2010).

385 However, some monazite zoning and textural relationships can be indicative of the
386 environment in which it formed. Pure sector-zoned monazite is likely common in igneous rocks
387 that have experienced little alteration (e.g., Cressey et al. 1999; Popova and Churin 2010). Sieve

388 textures are characteristic of authigenic monazite nodules (e.g., Burnotte et al. 1989; Milodowski
389 and Zalasiewicz 1991; Evans et al. 2002; Čopjaková et al. 2011). Grains that appear to have
390 undergone dissolution and reprecipitation reactions commonly show mottled overgrowths (e.g.,
391 Rasmussen and Muhling 2007; 2009; Mahan et al. 2010). Although rare, monazite has been
392 found as filling cracks in host minerals or along grain boundaries with apatite (e.g., Mathieu et
393 al. 2001; Catlos et al. 2008; Wawrzenitz et al. 2012), indicative of precipitation from a fluid
394 (Harlov et al. 2002; Harlov and Förster 2002; 2003; Harlov et al. 2005; Harlov 2011). Monazite
395 grains from ancient impact sites preserve fracture planes and granular textures characteristic of
396 high P metamorphism (Cavosie et al. 2010). Surfaces of individual monazite grains can also
397 indicate corrosion textures associated with fluids (Vavra and Schaltegger 1999). Baker et al.
398 (2008) report fibrous monazite grains from a garnet-bearing metapelite from western Turkey.
399 The garnet shows considerable internal zonation, consistent with multiple episodes of growth
400 and retrogression and the monazite grains likely experienced significant alteration.
401 Because of the nature of compositional substitutions (e.g., Table 2), primary monazite
402 can show a variety of shapes depending on its chemistry, which may be ideal for pinpointing
403 their origin (see examples in Popova and Churin 2010; Dill et al. 2012), although Montel et al.
404 (2011) found the shape and size of detrital monazite the "least useful" in identifying provenance.
405 Low-Th monazite may form a different morphology than high-Th grains (Fig. 7; Cressey et al.
406 1999). In primary low-Th monazite from a carbonatite, eight single crystal sectors develop with
407 La concentrated in {011} sectors and Nd, Pr, and other mid-REE are present in higher amounts
408 in {$\bar{1}$01} and {100}. In addition, low-Th monazites appear to have growth rates faster
409 perpendicular to the {011} direction relative to {$\bar{1}$01} and {100}. Sr will also concentrate in the
410 {100} sectors, whereas Ce is relatively constant across sectors. Thorium-rich (9-16 ThO_2 wt %)

sector-zoned monazite from granitic pegmatites do not follow these trends, with Ce enrichment found along some surfaces (e.g., Popova and Churin 2009). The presence of higher amounts of Th changes monazite morphology as crystals become flattened on {100}, show smaller {$\bar{1}$01} faces, and may not develop the {011} sectors (Fig. 7) (Cressey et al. 1999). This observation suggests that the Th content of the environment in which the mineral is crystallizing plays an important role in determining the morphology of monazite.

DISCUSSION

Monazite is typically a Th-rich mineral, with a number of possible substitution mechanisms allowing access for this radiogenic element to be incorporated into its structure (Table 2). Zoning of Th in monazite varies and is likely controlled by precursor reactants (e.g., allanite or REE oxides), P-T conditions, and the extent of fluid-rock interactions. These factors play major roles in controlling Th composition, as opposed to its crystal chemistry or its inclusion of other elements, like REE. Chondrite-normalized REE patterns of Himalayan monazite with allanite are similar (Figure 4), indicating that the reactant (allanite) controls the composition of product (monazite) in these metamorphic rocks. Note that the REE contents of the Himalayan monazites and their presence are independent of whole rock chemistry (Figure 5).

Any correlations between the amount of Th in monazite and metamorphic grade may be coincidental, but authigenic monazite typically contains low ThO_2. Monazite Th content is independent of that of silicate melts, but carbonatites typically contain low ThO_2 monazite. Thorium-rich patches and/or variable compositions likely reflect fluid-induced alteration; many low ThO_2 grains affected by fluids have been reported. Thorium-rich monazite is also no more susceptible to alteration than Th-poor accessory minerals. The long half-life of Th may be partly responsible for the ability of monazite to remain intact over long geological timescales.

Generalizations about Pb in monazite advocated by experimentalists contradict those working with natural samples. For example, one reason for the discrepancy in closure temperature reported by studies of Pb diffusion in monazite has been attributed to the difference in the behavior of natural and synthetic grains. Common Pb has been measured during the analysis of natural monazite grains using ion microprobe and isotope dilution techniques, but incorporating Pb into the monazite structure has been difficult to produce experimentally. Lead likely exists in monazite in its 2+ oxidation state and this cation is larger than others that can reside in its structure in 9-fold coordination (Table 3). Monazite grains from ore and/or hydrothermal deposits show higher amounts of the non-radiogenic Pb, which may provide clues into the conditions at which Pb incorporation into the mineral lattice is possible. Common Pb can be introduced via hydrothermal fluids, but other mechanisms may exist.

Correlations exist in some rocks between Y content and monazite age, but to generalize that all monazite grains will show this relationship ignores the potential for a complex reaction history for the rock and a range of potential sources of Y, which include the breakdown of accessory minerals (e.g., allanite, xenotime, and/or rare-earth oxides) and/or major minerals considered sinks for Y (e.g., garnet). When a relationship is observed between Y and age, the rock likely experienced a unique set of P-T and fluid conditions and considerable insight can be gained into its tectonic history. X-ray mapping of Y in garnet and monazite can assist in identifying the chemical relationship between these minerals.

The inability to develop a consistent language and identify effective descriptors of monazite zoning can be problematic because the appearance of the mineral can shed significant insight into its potential origin and degree of interaction with fluids. The monazite structure is flexible in that it can incorporate a large variety of cations and lattice distortions. The external

morphology of euhedral monazite crystals can be influenced by Th content (Fig. 7). Monazite grains are commonly zoned. Zoning is a function of crystal structure, what elements are present when the monazite grain forms or is altered, and the P-T and fluid conditions during formation or alteration. The mineral can crystallize initially with primary sector zoning, but the grains can be altered by secondary reactions. Authigenic and metasomatic monazite develop textures specific to these environments, but generalizations that insist that specific types of monazite zoning (Table 1) are restricted to igneous or metamorphic environments should be avoided because exceptions exist. Correlating mineral zoning in BSE images to the abundance of a specific element, like Th or Y, can be done using high-resolution X-ray element mapping or generating quantitative chemical data. A range of elements can display different types of zoning within single grains and contribute to mineral appearance in BSE images.

Although much has been done in terms of understanding the behavior of monazite, key controversies remain, including the influence of the mineral's chemistry and/or structure on controlling the diffusion of Pb and the reason for the occurrence of monazite grains with larger amounts of non-radiogenic Pb. Reactant availability, open system behavior, and the preference of the mineral structure in determining the composition of monazite is exemplified by its Y content. Competition between the breakdown of accessory and major minerals that contain elements necessary for monazite growth can complicate the mineral's chemistry in garnet-bearing assemblages. Some attribute monazite composition to its provenance, and these generalizations may be effective for a given field area and specific system that is being studied, but to transfer them to a general understanding of monazite behavior can be problematic and incorrect.

ACKNOWLEDGEMENTS

Comments from Drs. Dan Harlov, Michael Williams, and Gregory Dumond greatly improved the original manuscript. Samples analyzed in this study were collected and analyzed with the support of the National Science Foundation.

REFERENCES CITED

Aleinikoff, J.N., Burton, W.C., Lyttle, P.T., Nelson, A.E., and Southworth, S. (2000) U-Pb geochronology of zircon and monazite from Mesoproterozoic granitic gneisses of the northern Blue Ridge, Virginia and Maryland, USA. Precambrian Research, 99, 113-146.

Aleinikoff, J.N., Hayes, T.S., Evans, K.V., Mazdab, F.K., Pillers, R.M., and Fanning, C. (2012) SHRIMP U-Pb Ages of xenotime and monazite from the Spar Lake Red Bed-associated Cu-Ag Deposit, Western Montana: Implications for ore genesis. Economic Geology, 107, 1251-1274.

Aleinikoff, J.N., Schenck, W.S., Plank, M.O., Srogi, L., Fanning, C.M., Kamo, S.L., and Bosbyshell, H. (2006) Deciphering igneous and metamorphic events in high-grade rocks of the Wilmington Complex, Delaware: Morphology, cathodoluminescence and backscattered electron zoning, and SHRIMP U-Pb geochronology of zircon and monazite. Geological Society of America Bulletin, 118, 39-64.

Amli, R. (1975) Mineralogy and rare earth geochemistry of apatite and xenotime from the Gloserheia granite pegmatite, Froland, southern Norway. American Mineralogist, 60, 607-620.

Andrehs, G. and Heinrich, W. (1998) Experimental determination of REE distributions between monazite and xenotime: Potential for temperature-calibrated geochronology. Chemical Geology, 149, 83-96.

Ayers, J.C., Loflin, M., Miller, C.F., Barton M.D., and Coath, C.D. (2006) In situ oxygen isotope analysis of monazite as a monitor of fluid infiltration during contact metamorphism: Birch Creek Pluton aureole, White Mountains eastern California. Geology, 34, 654-656.

Ayers, J.C., Miller, C., Gorisch, B., and Milleman, J. (1999) Textural development of monazite during high-grade metamorphism: Hydrothermal growth kinetics, with implications for U,Th-Pb geochronology. American Mineralogist, 84, 1766-1780.

Baker, C.B., Catlos, E.J., Sorensen, S.S., Cemen, I., and Hancer, M. (2008) Evidence for polymetamorphic garnet growth in the Çine (southern Menderes) Massif, Western Turkey. IOP Conf. Series: Earth and Environmental Science, 2, 012020 doi:10.1088/1755-1307/2/1/012020.

Bea F. (1996) Residence of REE, Y, Th and U in granites and crustal protoliths: Implications for the chemistry of crustal melts. Journal of Petrology, 37, 521-552.

Beall, G.W., Boatner, L.A., Mullica, D.F., and Milligan, W.O. (1981) The structure of cerium ortho-phosphate, a synthetic analog of monazite. Journal of Inorganic and Nuclear Chemistry, 43, 101-105.

Bearss, G.T. and Pitman, L.C. (1996) Monazite-(Ce) from the Buckwheat dolomite at Franklin, New Jersey. The Mineralogical Record, 27.6, 439.

Berger A., Gnos, E., Janots, E., Fernandez, A., and Giese, J. (2008) Formation and composition of rhabdophane, bastnäsite and hydrated thorium minerals during alteration: Implications for geochronology and low-temperature processes. Chemical Geology, 254, 238-248.

Bernard-Griffiths, J., Peucat, J.J., Cornichet, J.J., Ponce de Leon, M.I., and Ibarguchi, J.I.G. (1985) U-Pb, Nd Isotope and REE geochemistry in eclogites from the Cabortegal

524 complex, Galicia, Spain: An example of REE immobility conserving MORB-like patterns
525 during high-grade metamorphism. Chemical Geology, 52, 217-225.
526 Black, L.P., Fitzgerald, J.D., and Harley, S.L. (1984) Pb isotopic composition, colour, and
527 microstructure of monazites from a polymetamorphic rock in Antarctica. Contributions to
528 Mineralogy and Petrology, 85, 141-148.
529 Boatner, L.A. and Sales, B.C. (1988) Radioactive waste forms for the future: monazite. In: W.
530 Lutze, R.C. Ewing, Ed., Radioactive Waste Forms for the Future, p.495-564, North-
531 Holland Publishers, Amsterdam.
532 Boggs, K.J. E., Kamo, S.L. Simony, P. Moore, J., and Archibald, D. (2002) A comparison of
533 CHIME and ID-TIMS U-Pb monazite ages from the Rocky Mountain Trench near
534 Golden, British Columbia, Canada and the importance of CHIME analyses. Abstracts
535 with Programs, Geological Society of America, 34, 68.
536 Bonyadi, Z., Davidson, G.J., Mehrabi, B., Meffre, S., and Ghazban, F. (2011) Significance of
537 apatite REE depletion and monazite inclusions in the brecciated Se-Chahun iron oxide-
538 apatite deposit, Bafq district, Iran: Insights from paragenesis and geochemistry. Chemical
539 Geology, 281, 253-269.
540 Bowie, S.H.U. and Horne, J.E.T. (1953) Cheralite a new mineral of the monazite group.
541 Mineralogical Magazine, 30, 93-99.
542 Breiter, K., Čopjaková , R., and Skoda, R. (2009) The involvement of F,CO_2, and As in the
543 alteration of Zr-Th-REE bearing accessory minerals in the Hora Svate Kateriny A-type
544 granite, Czech Republic. The Canadian Mineralogist, 47, 1375-1398.

545 Broska, I., Petrik, I., and Williams, C.T., 2000. Coexisting monazite and allanite in peraluminous
546 granitoids of the Tribec Mountains, Western Carpathians. American Mineralogist, 85, 22-
547 32.
548 Brouand, M. and Cuney, M. (1990) Substitution des radioe´le´ments dans la monazite des
549 granites hyperalumineux. Conse´quences pour la de´finition de leur potentialite´
550 me´talloge´nique. Bulletin de la Socie´te´ Franc¸aise de Mine´ralogie et de
551 Cristallographie, 2/3, 124-125.
552 Bruguier, O., Hammor, D., Bosch, D., and Caby, R. (2009) Miocene incorporation of peridotite
553 into the Hercynian basement of the Maghrebides (Edough massif, NE Algeria):
554 Implications for the geodynamic evolution of the Western Mediterranean. Chemical
555 Geology, 261, 172-184.
556 Burnotte, E., Pirard, E., and Michel, G. (1989) Genesis of gray monazites: Evidence from the
557 Paleozoic of Belgium. Economic Geology, 84, 1417-1429.
558 Burt, D.M. (1989) Compositional and phase relations among rare earth elements. In
559 Geochemistry and mineralogy of rare earth elements. In B.R. Lipin and G.A. McKay,
560 Eds., Reviews in Mineralogy, 21, Mineralogical Society of America, pp. 259-307.
561 Cabella, R., Lucchetti, G., and Marescotti, P. (2001) Authigenic monazite and xenotime from
562 pelitic metacherts in pumpellyite-actinolite-facies conditions, Sestri-Voltaggio Zone,
563 Central Liguria, Italy. The Canadian Mineralogist, 39, 717-727.
564 Catlos, E.J. (2000). Geochronologic and thermobarometric constraints on the evolution of the
565 Main Central Thrust, Himalayan orogen. PhD Thesis. University of California.
566 Catlos, E.J., Baker, C., Sorensen, S.S., Çemen, I., and Hancer, M. (2010) Geochemistry,
567 geochronology, and cathodoluminescence imagery of the Salihli and Turgutlu granites

(central Menderes Massif, western Turkey): Implications for Aegean tectonics. Tectonophysics, 488, 110-130.

Catlos, E.J. and Cemen, I. (2005) Monazite ages and rapid exhumation of the Menderes Massif, western Turkey. International Journal of Earth Sciences, 94, 204-217.

Catlos, E.J., Dubey, C.S., and Sivasubramanian, P. (2008) Monazite ages from carbonatites and high-grade assemblages along the Kambam Fault Southern Granulite Terrain, South India. American Mineralogist, 93, 1230-1244.

Catlos, E.J., Gilley, L.D., and Harrison, T.M. (2002) Interpretation of monazite ages obtained via in situ analysis. Chemical Geology, 188, 193-215.

Catlos, E.J., Harrison, T.M., Kohn, M.J., Grove, M., Ryerson, F.J., Manning, C.E., and Upreti, B.N. (2001) Geochronologic and thermobarometric constraints on the evolution of the Main Central Thrust, central Nepal Himalaya. Journal of Geophysical Research, 106, 16177-16204.

Cavosie, A.J., Quintero, R.R., Radovan, H.A., and Moser D.E. (2010) A record of ancient cataclysm in modern sand: Shock microstructures in detrital minerals from the Vaal River, Vredefort Dome, South Africa. Geological Society of America Bulletin, 122, 1968-1980.

Chatterjeea, N., Banerjeeb, M., Bhattacharyab, A., and Majic A.K. (2010) Monazite chronology, metamorphism-anatexis and tectonic relevance of the mid-Neoproterozoic Eastern Indian Tectonic Zone. Precambrian Research, 179, 99-120.

Chen, C-H., Liu, Y-H., Lee, C-Y., Xiang, H., and Zhou, H-W. (2012) Geochronology of granulite, charnockite and gneiss in the poly-metamorphosed Gaozhou Complex (Yunkai

590 massif), South China: Emphasis on the in-situ EMP monazite dating. Lithos, 144-145,
591 109-129.
592 Cherniak, D.J. (2010) Diffusion in Accessory Minerals: Zircon, Titanite, Apatite, Monazite and
593 Xenotime. Reviews in Mineralogy and Geochemistry, 72, 827-869.
594 Cherniak, D.J. and Pyle, J.M. (2008) Thorium diffusion in monazite. Chemical Geology, 256,
595 52-61.
596 Cherniak, D.J., Watson, E.B., Grove, M., and Harrison, T.M. (2004) Pb diffusion in monazite: a
597 combined RBS/SIMS study. Geochimica et Cosmochimica Acta 68, 829-840.
598 Choo, C.O. (2002) Complex compositional zoning in epidote from rhyodacitic tuff, Bobae
599 sericite deposit, southeastern Korea. Nues Jahrbuch für Mineralogie, 177, 181-197.
600 Choo, C.O. (2003) Mineralogical studies on complex zoned tourmaline in diaspore nodules from
601 the Milyang clay deposit, Korea. Geosciences Journal, 7, 151-156.
602 Clavier, N., Podor, R., and Dacheux, N. (2011) Crystal chemistry of the monazite structure.
603 Journal of the European Ceramic Society, 31, 941-976.
604 Čopjaková , R., Novak, M., and Francu, E. (2011) Formation of authigenic monazite-(Ce) to
605 monazite-(Nd) from Upper Carboniferousgraywackes of the Drahany Upland: Roles of
606 the chemical composition of host rock and burial temperature. Lithos, 127, 373-385.
607 Corfu, F. (1988) Differential response of U-Pb systems in coexisting accessory minerals,
608 Winnipeg River Subprovince, Canadian Shield: implications for Archean crustal growth
609 and stabilization. Contributions to Mineralogy and Petrology, 98, 312-325.
610 Cressey, G., Wall, I.F., and Cressey, B.A. (1999) Differential REE uptake by sector growth of
611 monazite. Mineralogical Magazine, 63, 813-828.

612 Crowley, J.L., Brown, R.L., Gervais, F., and Gibson, H.D. (2008) Assessing inheritance of
613 zircon and monazite in granitic rocks from the Monashee Complex, Canadian Cordillera.
614 Journal of Petrology, 49, 1915-1929.
615 Crowley, J.L. and Ghent, E.D. (1999) An electron microprobe study of the U-Th-Pb systematics
616 of metamorphosed monazite: the role of Pb diffusion versus overgrowth and
617 recrystallization. Chemical Geology, 157, 285-302.
618 Dahl, P.S., Hamilton, M.A., Jercinovic, M.J., Terry, M.P., Williams, M.L. and Frei, R. (2005)
619 Comparative isotopic and chemical geochronometry of monazite, with implications for
620 U-Th-Pb dating by electron microprobe: an example from metamorphic rocks of the
621 eastern Wyoming Craton (U.S.A.). American Mineralogist, 90, 619-638.
622 Dana, J.D., Dana, E.S., Palach, Ch., Berman, G. and Frondel, K. (1951) System of Mineralogy.
623 Vol. 2 (Wiley, New York, 1951; Inostrannaya Literatura, Moscow, 1954).
624 Dawood, Y.H., and El-Naby, H.H. (2007) Mineral chemistry of monazite from the black sand
625 deposits, northern Sinai, Egypt: a provenance perspective. Mineralogical Magazine, 71,
626 389-406.
627 Deer, W.A., Howie, R.A., and Zussman, J. (1992) An Introduction to the Rock-Forming
628 Minerals (2nd Edition). Prentice Hall, New York, 712pp.
629 Della Ventura, G., Mottana, A., Parodi, G.C., Raudsepp, M., Bellatreccia, F., Caprilli, E., Rossi,
630 P., and Fiori, S. (1996) Monazite-huttonite solid-solutions from the Vico Volcanic
631 Complex, Latium, Italy. Mineralogical Magazine, 60, 751-758.
632 Demartin, F., Pilati, T., Diella, V., Donzelli, S., Gentile, P., and Gramaccioli, C.M. (1991a) The
633 chemical composition of xenotime from fissures and pegmatites in the Alps. The
634 Canadian Mineralogist, 29, 69-75.

635 Demartin, F., Pilati, T., Diella, V., Donzelli, S., and Gramaccioli, C.M. (1991b) Alpine monazite:
636 Further data. The Canadian Mineralogist, 29, 61-67.
637 DeWolf, C.P., Belshaw, N., and O'Nions, R.K. (1993) A metamorphic history from micron-scale
638 ^{207}Pb-^{206}Pb chronometry of Archean monazite. Earth and Planetary Science Letters, 120,
639 207-220.
640 Dill, H.G., Weber, B., and Klosa, D. (2012) Morphology and mineral chemistry of monazite-
641 zircon-bearing stream sediments of continental placer deposits (SE Germany): Ore guide
642 and provenance marker. Journal of Geochemical Exploration, 112, 322-346.
643 Dowty, E. (1976) Crystal structure and crystal growth: II. Sector zoning in minerals. American
644 Mineralogist, 61, 460-469.
645 Dubrail, J., Farges, F., Gautron, L., Harfouche, M., Borca, C., and Grolimund, D. (2009) Pb in
646 naturally irradiated monazites and zircons. Journal of Physics: Conference Series, 190,
647 012180, doi:10.1088/1742-6596/190/1/012180.
648 Evans, J.A., Zalasiewicz, J.A., Fletcher, I., Rasmussen, B., and Pearce, N.J.G. (2002) Dating
649 diagenetic monazite in mudrocks: constraining the oil window? Journal of the Geological
650 Society, London, 159, 619-622.
651 Exley, R.A. (1980) Microprobe studies of REE-rich accessory minerals: Implications for Skye
652 granite petrogenesis and REE mobility in hydrothermal systems. Earth and Planetary
653 Science Letters, 48, 97-110.
654 Faure, M., Mezeme, E.B., Cocherie, A., Rossi, P., Chemenda, A., and Boutelier, D. (2008)
655 Devonian geodynamic evolution of the Variscan Belt, insights from the French Massif
656 Central and Massif Armoricain. Tectonics, 27, TC2005, doi:10.1029/2007TC002115.

Felsche, J. (1976) Yttrium and lanthanides, section A. In K. H. Wedepohl, Ed., Handbook of Geochemistry, v.II, section 39, 57-71, p. Al-A42.

Förster, H.J. (1998) The chemical composition of REE-Y-Th-Urich accessory minerals in peraluminous granites of the Erzgebirge-Fichtelgebirge region, Germany: Part I. The monazite-(Ce)-brabantite solid solution series. American Mineralogist, 83, 259-272.

Förster , H.J. and Harlov, D.E. (1999) Monazite-(Ce) huttonite solid solutions in granulite-facies metabasites from the Ivrea-Verbano Zone, Italy. Mineralogical Ma**g**azine, 63, 587-594.

Foster, G., Gibson, H.D., Parrish, R., Horstwood, M., Fraser, J., and Tindle, A. (2002) Textural, chemical and isotopic insights into the nature and behaviour of metamorphic monazite Chemical Geology, 191, 183- 207.

Frei, R., Villa, I.M., Nagler, Th-F., Kramers, J.D., Przybylowicz, W.J., Prozesky, V.M., Hofmann, B.A., Kamber, B.S. (1997) Single mineral dating by the Pb-Pb step-leaching method: Assessing the mechanisms. Geochimica et Cosmochimica Acta, 61, 393-414.

Gagne, S., Jamieson, R.A., MacKay, R., Wodicka, N., and Corrigan, D. (2009) Texture, composition, and age variations in monazite from the lower amphibolite to the granulite facies Longstaff Bluff formation, Baffin Island, Canada. The Canadian Mineralogist, 47, 847-869.

Gardes, E., Jaoul, O., Montel, J.M., Seydoux-Guillaume, A.M., and Wirth R. (2006) Pb diffusion in monazite: an experimental study of $Pb^{2+} + Th^{4+} \leftrightarrow 2Nd^{3+}$ interdiffusion. Geochimica et Cosmochimica Acta, 70, 2325-2336.

Gasser, D., Bruand, E., Rubatto, D., and Stuwe, K. (2012) The behaviour of monazite from greenschist facies phyllites to anatectic gneisses: An example from the Chugach Metamorphic Complex, southern Alaska. Lithos, 134-135, 108-122.

680 Gibson, H.D., Carra, S.D., Brown, R.L., and Hamilton, M.A. (2004) Correlations between
681 chemical and age domains in monazite, and metamorphic reactions involving major
682 pelitic phases: an integration of ID-TIMS and SHRIMP geochronology with Y-Th-U X-
683 ray mapping. Chemical Geology, 211, 237-260.
684 Giere, R., Rumble, D., Gunther, D., Connolly, J., and Caddick, M.J. (2011) Correlation of
685 growth and breakdown of major and accessory minerals in metapelites from
686 Campolungo, Central Alps. Journal of Petrology, 52, 2293-2334.
687 Glodny, J. and Hetzel, R. (2007) Precise U-Pb ages of syn-extensional Miocene intrusions in the
688 central Menderes Massif, western Turkey. Geological Magazine, 144, 235-246.
689 Goncalves, P., Williams, M.I., and Jercinovic, M.J. (2005) Electron-microprobe age mapping of
690 monazite. American Mineralogist, 90, 578-585.
691 Gramaccioli, C.M. and Segalstad, T.V. (1978) A uranium- and thorium-rich monazite from
692 south-alpine pegmatite at Piona, Italy. American Mineralogist, 63, 757-761.
693 Gratz, R. and Heinrich, W. (1997) Monazite-xenotime thermobarometry: Experimental
694 calibration of the miscibility gap in the binary system $CePO_4$-YPO_4. American
695 Mineralogist, 82, 772-780.
696 Gratz, R. and Heinrich, W. (1998) Monazite-xenotime thermometry: III. Experimental
697 calibration of the partitioning of gadolinium between monazite and xenotime. European
698 Journal of Mineralogy, 10, 579-588.
699 Grove, M. and Harrison, T.M. (1999) Monazite Th-Pb age depth profiling Geology, 27, 487-490.
700 Harlov, D. (2011) Petrological and experimental application of REE- and actinide-bearing
701 accessory minerals to the study of Precambrian high-grade gneiss terranes. Geological
702 Society of America Memoirs, 207, 13-24.

703 Harlov, D.E., and Förster, H.-J. (2002) High-grade fl uid metasomatism on both a local and
704 regional scale: The Seward Peninsula, Alaska, and the Val Strona di Omegna, Ivrea-
705 Verbano Zone, northern Italy. Part I: Petrography and silicate mineral chemistry. Journal
706 of Petrology, 43, 769-799.
707 Harlov, D.E., and Förster, H.-J. (2003) Fluid-induced nucleation of (Y+REE)-phosphate
708 minerals within apatite: Nature and experiment. Part II. Fluorapatite. American
709 Mineralogist, 88, 1209-1229.
710 Harlov, D.E., Förster, H.-J., and Nijland, T.G. (2002) Fluid-induced nucleation of (Y + REE)-
711 phosphate minerals within apatite: Nature and experiment. Part I. Chlorapatite. American
712 Mineralogist, 87, 245-261.
713 Harlov, D.E. and Hetherington, C.J. (2010) Partial high-grade alteration of monazite using alkali-
714 bearing fluids: experiment and nature. American Mineralogist, 95, 1105-1108.
715 Harlov, D.E., Wirth, R., and Förster, H.-J. (2005) An experimental study of dissolution-
716 reprecipitation in fluorapatite: fluid infiltration and the formation of monazite.
717 Contributions to Mineralogy and Petrology, 150, 268-286.
718 Harlov, D.E., Wirth, R., and Hetherington, C.J. (2007) The relative stability of monazite and
719 huttonite at 300-900 °C and 200-1000 MPa: metasomatism and the propagation of
720 metastable mineral phases. American Mineralogist, 92, 1652-1664.
721 Harlov, D.E., Wirth, R., and Hetherington, C.J. (2011) Fluid-mediated partial alteration in
722 monazite: the role of coupled dissolution-reprecipitation in element redistribution and
723 mass transfer. Contributions to Petrology and Mineralogy, 162, 329-348.
724 Harrison, T.M., Catlos, E.J., and Montel, J-M. (2002) U-Th-Pb Dating of Phosphate Minerals.
725 In: J.M. Hughes, M. Kohn and J. Rakovan, Eds., Phosphates: Geochemical,

726 Geobiological and Materials Importance. Mineralogical Society of America, Washington
727 D.C., pp. 523-558.
728 Hawkins, D.P. and Bowring, S.A. (1997) U-Pb systematics of monazite and xenotime: case
729 studies from the Paleoproterozoic of the Grand Canyon, Arizona. Contributions to
730 Mineralogy and Petrology, 127, 87-103.
731 Hazen, R.M., Ewing, R.C., and Sverjensky, D.A. (2009) Evolution of uranium and thorium
732 minerals. American Mineralogist, 94, 1293-1311.
733 Heinrich, W., Andrehs, G., and Franz, G. (1997) Monazite-xenotime miscibility gap
734 thermometry. I. An empirical calibration. Journal of Metamorphic Geology, 15, 3-16.
735 Hietpas, J., Samson, S., and Moecher, D. (2011) A direct comparison of the ages of detrital
736 monazite versus detrital zircon in Appalachian foreland basin sandstones: Searching for
737 the record of Phanerozoic orogenic events. Earth and Planetary Science Letters, 310, 488-
738 497.
739 Hinchey, A.M., Carr, S.D., and Rayner, N. (2007) Bulk compositional controls on the
740 preservation of age domains within metamorphic monazite: A case study from quartzite
741 and garnet-cordierite-gedrite gneiss of Thor-Odin dome, Monashee complex, Canadian
742 Cordillera. Chemical Geology, 240, 85-102.
743 Hoisch, T.D., Wells, M.L., and Grove, M. (2008) Age trends in garnet-hosted monazite
744 inclusions from upper amphibolite facies schist in the northern Grouse Creek Mountains,
745 Utah. Geochimica et Cosmochimica Acta, 72, 5505-5520.
746 Hokada, T. and Motoyoshi, Y. (2006) Electron microprobe technique for U-Th-Pb and REE
747 chemistry of monazite, and its implications for pre-, peak-, and post-metamorphic events

748 pf the Lutzow-Holm Complex and the Napier Complex, East Antartica. Polar
749 Geoscience, 19, 118-151.
750 Honig, S., Leichmann, J., and Novak, M. (2010) Unidirectional solidification textures and garnet
751 layering in Y-enriched garnet-bearing aplite-pegmatites in the Cadomian Brno Batholith,
752 Czech Republic. Journal of Geosciences, 55, 113-129.
753 Huang, T, Lee, J-S., Kung, J., and Lin, C-M. (2010) Study of monazite under high pressure.
754 Solid State Communications, 150, 1845-1850.
755 Huminicki, D.M.C. and Hawthorne, F.C. (2002) The Crystal Chemistry of the Phosphate
756 Minerals. In: J.M. Hughes, M. Kohn and J. Rakovan, Eds., Phosphates: Geochemical,
757 Geobiological and Materials Importance. Mineralogical Society of America, Washington
758 D.C., pp 123-253.
759 Iizuka, T., McCulloch M.T., Komiya, T., Shibuya, T., Ohta, K., Ozawa, H., Sugimura, E., and
760 Collerson, K.D. (2010) Monazite geochronology and geochemistry of meta-sediments in
761 the Narryer Gneiss Complex, Western Australia: constraints on the tectonothermal
762 history and provenance. Contributions to Mineralogy and Petrology, 160, 803-823.
763 Ilupin, I. P., Khomyakov, A. P., and Balashov, Yu. A. (1971) Rare earths in accessory minerals
764 of Yakutian kimberlite. Doklady Akademii Nauk SSSR, 201,1214-1217 (transl. Doklady
765 of the Academy of Sciences of the U.S.S.R.,201,272- 274, 1971)
766 Janots, E., Berger, A., Gnos, E., Whitehouse, M., Lewin, E., and Pettke, T. (2012) Constraints on
767 fluid evolution during metamorphism from U-Th-Pb systematics in Alpine hydrothermal
768 monazite. Chemical Geology, 326-327, 61-71.

769 Kartashov, P.M., Bogatikov, O.A., Mokhov, A.V., Gorshkov, A.I., Ashikhmina, N. A.
770 Magazina, L.O., and Koporulina, E.V. (2006) Lunar monazites. Doklady Earth Sciences,
771 407A, 498-502.
772 Kelly, K.L., Beall, G.W.,Young, J.P., and Boatner, L.A. (1981) Valence states of actinides in
773 synthetic monazites. In J.G. Moore, Ed., The Scientific Basis For Nuclear Waste
774 Management 3, p. 189-195. Plenum, New York.
775 Kelly, N.M., Harley, S.L., and Möller, A. (2012) Complexity in the behavior and
776 recrystallization of monazite during high-T metamorphism and fluid infiltration.
777 Chemical Geology, 322-323, 192-208.
778 Kempe, U., Lehmann, B. Wolf, D., Rodionov, N., Bombach, K., Schwengfelder, U., and
779 Dietrich, A. (2008) U-Pb SHRIMP geochronology of Th-poor, hydrothermal monazite:
780 An example from the Llallagua tin-porphyry deposit, Bolivia. Geochimica et
781 Cosmochimica Acta, 72, 4352-4366.
782 Kohn, M.J. and Malloy, M.A. (2004) Formation of monazite via prograde metamorphic reactions
783 among common silicates: implications for age determinations. Geochimica et
784 Cosmochimica Acta, 68, 101-113.
785 Kohn, M.J. and Vervoot, J. D. (2008) U-Th-Pb dating of monazite by single-collector ICP-MS:
786 Pitfalls and potential. Geochemistry, Geophysics and Geosystems, 9, 1-16.
787 Krenn, E. and Finger, F. (2010) Unusually Y-rich monazite-(Ce) with 6-14 wt.% Y2O3 in a
788 granulite from the Bohemian Massif: implications for high-temperature monazite growth
789 from the monazite-xenotime miscibility gap thermometry. Mineralogical Magazine, 74,
790 217-225.

791 Krenn, E., Janak, M., Fritz, F., Broska I., and Konecny, P. (2009) Two types of metamorphic
792 monazite with contrasting La/Nd, Th and Y signature in a (ultra) high pressure metapelite
793 from the Pohorje Mountains, Slovenia: Indications for a pressuredependent REE
794 exchange between apatite and monazite? American Mineralogist, 94, 801-815.
795 Krenn, E., Putz, H., Finger, F., and Paa, W. (2008a) Unusual monazite with high S, Sr, Eu and
796 common Pb contents in ore bearing mylonites from the Schellgaden mining district,
797 Austria. EGU General Assembly Geophysical Research Abstracts, 10, EGU2008-A-
798 11796.
799 Krenn, E., Ustaszewski, K., and Finger, F. (2008b) Detrital and newly formed metamorphic
800 monazite in amphibolite-facies metapelites from the Motajica Massif, Bosnia. Chemical
801 Geology, 254, 164-174.
802 Krenn, E., Putz, H., Finger, F., and Paar, W.H. (2011) Sulfur-rich monazite with high common
803 Pb in ore-bearing schists from the Schellgaden mining district (Tauern Window, Eastern
804 Alps). Mineralogy and Petrology, 102, 51-62.
805 Kucha, H. (1980) Continuity in the monazite-huttonite series. Mineralogical Magazine, 43, 1031-
806 1034.
807 Kusiak M.A., Suzuki, K., Dunkley, D.J., Lekki, J., Bakun-Czubarow, N., Paszkowski, M., and
808 Budzyn, B. (2008) EPMA and PIXE dating of monazite in granulites from Stary
809 Gierałtów, NE Bohemian Massif, Poland. Gondwana Research, 14, 675-685.
810 Li, N., Chen, Y-J., Fletcher, I.R., and Zeng, Q-T. (2011) Triassic mineralization with Cretaceous
811 overprint in the Dahu Au-Mo deposit, Xiaoqinling gold province: Constraints from
812 SHRIMP monazite U-Th-Pb geochronology. Gondwana Research, 20, 543-552.

813 Lobato, L.M., Santos, J.O.S., McNaughton, N.J. Fletcher, I.R., and Noce, C.M. (2007) U-Pb
814 SHRIMP monazite ages of the giant Morro Velho and Cuiabá gold deposits, Rio das
815 Velhas greenstone belt, Quadrilátero Ferrífero, Minas Gerais, Brazil. Ore Geology
816 Reviews 32, 674-680.
817 Loomis, T.P. (1983) Compositional zoning of crystals: a record of growth and reaction history.
818 In: Saxena, S.K. (ed) Kinetics and equilibrium in mineral reactions (Advances in physical
819 geochemistry, vol 3). Springer, New York, pp 1-60.
820 Mahan, K.H., Goncalves, P., Williams, M.L., and Jercinovic, M.J. (2006) Dating metamorphic
821 reactions and fluid flow: application to exhumation of high-P granulites in a crustal-scale
822 shear zone, western Canadian Shield. Journal of Metamorphic Geology, 24, 193-217.
823 Mahan, K.H., Wernicke, B.P., and Jercinovic, M.J. (2010) Th-U-total Pb geochronology of
824 authigenic monazite in the Adelaide rift complex, South Australia, and implications for
825 the age of the type Sturtian and Marinoan glacial deposits. Earth and Planetary Science
826 Letters, 289, 76-86.
827 Majka, J., Beeri-Shlevin, Y., Geel, D.G., Ladenberger, A., Claesson, S., Konecny, P., and
828 Klonowskai, I. (2012) Multiple monazite growth in the Åreskutan migmatite: evidence
829 for a polymetamorphic Late Ordovician to Late Silurian evolution in the Seve Nappe
830 Complex of west-central Jämtland, Sweden. Journal of Geosciences, 57, 3-23.
831 Marsh, J.H., Grew, E.S., Gerbi, C.C., Yates, M.G., and Culshaw, N.G. (2012) The petrogenesis
832 of the garnet menzerite-(Y) in granulite facies rocks of the Parry Sound Domain,
833 Grenville Province, Ontario. The Canadian Mineralogist, 50, 73-99.

Martin, A.J., Gehrels, G.E., and DeCelles, P.G. (2007) The tectonic significance of (U,Th)/Pb ages of monazite inclusions in garnet from the Himalaya of central Nepal. Chemical Geology, 244, 1-24.

Martins, L., Vlach, S.R.F., and Janasi, V-dA. (2009) Reaction microtextures of monazite: Correlation between chemical and age domains in the Nazaré Paulista migmatite, SE Brazil. Chemical Geology, 261, 271-285.

Maslennikova, T.P., Osipov, A.V. Mezentseva L.P., Drozdova, I.A., Kuchaeva, S.K., Ugolkov, V. L., and Gusarov, V. V. (2010) Synthesis, mutual solubility, and thermal behavior of nanocrystals in the $LaPO_4$-YPO_4-H_2O system. Glass Physics and Chemistry, 36, 351-357.

Mathieu, R., Zetterstrom, L., Cuney, M., Gauthier-Lafaye, F., and Hidaka, H. (2001) Alteration of monazite and zircon and lead migration as geochemical tracers of fluid paleocirculations around the Oklo-Okelobondo and Bangombe natural nuclear reaction zones (Franceville basin, Gabon). Chemical Geology 171, 147-171.

McFarlane, C.R.M. and Harrison, T.M. (2006) Pb-diffusion in monazite: Constraints from a high-T contact aureole setting. Earth and Planetary Science Letters, 250, 376-384.

Meldrum, A., Boatner, L.A., Weber, W.J., and Ewing, R.C. (1998) Radiation damage in zircon and monazite. Geochimica et Cosmochimica Acta, 62, 2509-2520.

Milodowski, A.E. and Zalasiewicz, J.A. (1991) Redistribution of rare earth elements during diagenesis of turbidite/ hemipelagite mudrock sequences of Llandovery age from central Wales. In A. C. Morton, S.P. Todd, and P.D.W. Haughton, Eds., Developments in Sedimentary Provenance Studies. Geological Society Special Publication, 57, 101-124.

Mogilevsky, P. (2007) On the miscibility gap in monazite-xenotime systems. Physics and Chemistry of Minerals, 34, 201-214.

857 Mohr, D.W. (1984) Zoned porphyroblasts of metamorphic monazite in the Anakeesta Formation,
858 Great Smoky Mountains, North Carolina. American Mineralogist, 69, 98-103.
859 Mooney, R.C.L. (1948) Crystal Structures of a Series of Rare Earth phosphates. Journal of
860 Chemical Physics, 16, 1003, doi: 10.1063/1.1746668.
861 Montel, J-M., Foret, S., Veschambre, M., Nicollet, C., and Provost, A. (1996) Electron
862 microprobe dating of monazite. Chemical Geology, 131, 37-53.
863 Montel, J-M., Razafimahatratra, D., Ralison, B., De Parseval, P., Thibault, M., and Randranja, R.
864 (2011) Monazite from mountain to ocean: a case study from Trolognaro (Fort-Dauphin),
865 Madagascar. European Journal of Mineralogy, 23, 745-757.
866 Morelli, R.M., Bell, C.C., Creaser, R.A., and Simonetti, A. (2010) Constraints on the genesis of
867 gold mineralization at the Homestake Gold Deposit, Black Hills, South Dakota from
868 rhenium-osmium sulfide geochronology. Mineralium Deposita, 45, 461-480.
869 Ni, Y., Hughes, J.M., and Mariano, A.N. (1995. Crystal chemistry of the monazite and xenotime
870 structures. American Mineralogist, 80, 21-26.
871 Oelkers, E.H. and Poitrasson, F. (2002) An experimental study of the dissolution stoichiometry
872 and rates of a natural monazite as a function of temperature from 50 to 230 °C and pH
873 from 1.5 to 10. Chemical Geology, 191, 73-87.
874 Overstreet, W.C. (1967) The geological occurrence of monazite. U.S. Geological Survey
875 Progress Paper, 530.
876 Pan, Y. (1997) Zircon- and monazite-forming metamorphic reactions at Manitouwadge, Ontario.
877 The Canadian Mineralogist, 35, 105-118.

878 Panda, N.K., Rajagopalan, V., and Ravi, G.S. (2003) Rare-earth-element geochemistry of placer
879 monazites from Kalingapatnam Coast, Srikakulam District, Andhra Pradesh. Journal of
880 the Geological Society of India, 62, 429-438.
881 Parrish, R.R. (1990) U-Pb dating of monazite and its application to geological problems.
882 Canadian Journal of Earth Science, 27, 1431-1450.
883 Pe-pier, G. and McKay, R.M. (2006) Provenance of Lower Cretaceous sandstones onshore and
884 offshore Nova Scotia from electron microprobe geochronology and chemical variation of
885 detrital monazite. Bulletin of Canadian Petroleum Geology, 54, 366-379.
886 Petrik, I. and Konecny, P. (2009) Metasomatic replacement of inherited metamorphic monazite
887 in a biotite-garnet granite from the Nízke Tatry Mountains, Western Carpathians,
888 Slovakia: Chemical dating and evidence for disequilibrium melting. American
889 Mineralogist, 94, 957-974.
890 Pilipiuk A.N., Ivanikov V.V., and Bulakh A.G. (2001) Unusual rocks and mineralisation in a
891 new carbonatite complex at Kandaguba, Kola Peninsula, Russia. Lithos, 56, 333-347.
892 Podor R. (1994) Synthèse et caractérisation des monazites uranifères et thorifères. PhD thesis of
893 Université Henri Poincaré, Nancy (France).
894 Podor R. and Cuney M. (1997) Experimental study of Th-bearing LaPO4 (780 ◦C, 200MPa):
895 implications for monazite and actinide orthophosphate stability. American Mineralogist,
896 82, 765-771.
897 Poitrasson, F., Chenery, S., and Shepherd, T.J. (2000) Electron microprobe and LA-ICP-MS
898 study of monazite hydrothermal alteration: Implications for U-Th-Pb geochronology and
899 nuclear ceramics: Geochimica et Cosmochimica Acta, 64, 3283-3297.

900 Popova, V.I., and Churin, E. I. (2010) Zoning and sectoriality of monazite-(Ce) from granite
901 pegmatites of the central and south Urals. Geology of Ore Deposits, 52, 646-655.
902 Pršek, J., Ondrejka, M., Bačík, P., Budzyń, B., and Uher, P. (2010) Metamorphic-hydrothermal
903 REE minerals in the Bacúch magnetite deposit, western Carpathians, Slovakia: (Sr, S)-
904 rich monazite-(Ce) and Nd-dominant hingganite. The Canadian Mineralogist, 48, 81-94.
905 Pyle, J.M. and Spear, F.S. (2003) Four generations of accessory-phase growth in low-pressure
906 migmatites from SW New Hampshire. American Mineralogist, 88, 338-351.
907 Pyle, J.M., Spear, F.S., Rudnick, R.L., and McDonough, W.F. (2001) Monazite-xenotime-garnet
908 equilibria in metapelites and a new monazite-garnet thermometer. Journal of Petrology
909 42, 2083- 2107.
910 Quarton, M., Zouiri, M., and Freundlich,W. (1984) Cristallochimie des orthophosphates doubles
911 de thorium et de plomb. C R Acad Sci Ser II, 299, 785-788.
912 Rasmussen, B. and Muhling, J.R. (2007) Monazite begets monazite: evidence for dissolution of
913 detrital monazite and reprecipitation of syntectonic monazite during lowgrade regional
914 metamorphism. Contributions to Mineralogy and Petrology 154, 675-689.
915 Rasmussen, B. and Muhling, J.R. (2009) Reactions destroying detrital monazite in greenschist-
916 facies sandstones from the Witwatersrand basin, South Africa. Chemical Geology, 264,
917 311-327.
918 Rasmussen, B., Fletcher, I.R., and Muhling, J.R. (2007) In situ U-Pb dating and element
919 mapping of three generations of monazite: unravelling cryptic tectonothermal events in
920 low-grade terranes. Geochimica et Cosmochimica Acta, 71, 670-690.

921 Regis, D., Cenki-Tok, B., Darling, J., and Engi, M. (2012) Redistribution of REE, Y, Th, and U
922 at high pressure: Allanite-forming reactions in impure meta-quartzites (Sesia Zone,
923 Western Italian Alps). American Mineralogist, 97, 315-328.
924 Reno, B.L., Piccoli, P.M., Brown, M., and Trouw, R.A.J. (2012) In situ monazite (U-Th)-Pb ages
925 from the Southern Brasılia Belt, Brazil: constraints on the high-temperature retrograde
926 evolution of HP granulites. Journal of Metamorphic Geology, 30, 81-112.
927 Rubatto, D., Hermann, J., and Buick, I.S. (2006) Temperature and bulk composition control on
928 the growth of monazite and zircon during low-pressure anatexis (Mount Stafford, Central
929 Australia). Journal of Petrology, 47, 1973-1996.
930 Sano, Y., Takahata, N., Tsutsumi, Y., and Miyamoto, T. (2006) Ion microprobe U-Pb dating of
931 monazite with about five micrometer spatial resolution. Geochemical Journal, 40, 597-
932 608.
933 Santosh, M., Collins, A.S., Tamashiro, I., Koshimoto, S., Tsutsumi, Y., and Yokoyama, K.
934 (2006) The timing of ultrahigh-temperature metamorphism in Southern India: U-Th-Pb
935 electron microprobe ages from zircon and monazite in sapphirine-bearing granulites.
936 Gondwana Research, 10, 128-155.
937 Schandl, E.S. and Gorton, M.P., 2004, A textural and geochemical guide to the identification of
938 hydrothermal monazite: Criteria for selection of samples for dating epigenetic
939 hydrothermal ore deposits: Economic Geology and Bulletin of the Society of Economic
940 Geologists, 99, 1027-1035.
941 Semenov, E.I. (2001) REE, Th, and U mineralization and ores (Lanthanides and Actinides)
942 (GEOS, Moscow) [in Russian].

943 Seydoux-Guillaume, A.-M., Montel, J.-M., Bingen, B., Bosse, V., de Parseval, P., Paquette, J.-
944 L., Janots, E., and Wirth, R. (2012) Low-temperature alteration of monazite: Fluid
945 mediated coupled dissolution-precipitation, irradiation damage, and disturbance of the U-
946 Pb and Th-Pb chronometers. Chemical Geology, 330-331, 140-158.
947 Seydoux-Guillaume, A.-M., Paquette, J.-L., Wiedenbeck, M., Montel, J.-M., and Heinrich, W.
948 (2002b) Experimental resetting of the U-Th-Pb systems in monazite: Chemical Geology,
949 191, 165-181.
950 Seydoux-Guillaume, A. M., Wirth, R., Nasdala, L., Gottschalk, M. Montel, J. M., and Heinrich
951 W. (2002a) An XRD, TEM and Raman study of experimentally annealed natural
952 monazite. Phys Chem Minerals, 29, 240-253.
953 Shannon, R.D. (1976) Revised effective ionic radii and systematic studies of interatomie
954 distances in halides and chaleogenides. Acta Crystallographica, A32, 751-767.
955 Shaw, D.M. (1956) Geochemistry of pelitic rocks: Part III. Major elements and general
956 geochemistry. Bulletin of the Geological Society of America 67, 919-934.
957 Shaw, C.A., Karlstrom, K.E., Williams, M.L., Jercinovic, M.J., and McCoy, A.M. (2001)
958 Electron-microprobe monazite dating of ca. 1.71-1.63 Ga and ca. 1.45-1.38 Ga
959 deformation in the Homestake shear zone, Colorado: Origin and early evolution of a
960 persistent intracontinental tectonic zone. Geology, 29, 739-742.
961 Sheard, E.R., Williams-Jones, A.E., Heiligmann, M., Pederson, C., and Trueman, D.L. (2012)
962 Controls on the Concentration of Zirconium, Niobium, and the Rare Earth Elements in
963 the Thor Lake Rare Metal Deposit, Northwest Territories, Canada. Economic Geology,
964 107, 81-104.

965 Shtukenberg, A.G., Punin, Y.O., and Artamonova, O.I. (2009) Effect of crystal composition and
966 growth rate on sector zoning in solid solutions grown from aqueous solutions.
967 Mineralogical Magazine, 73, 385-398.
968 Sindern, S., Gerdes, A., Ronkin, Y.L., Dziggel, A., Hetzel, R., and Schulte, B.A. (2012).
969 Monazite stability, composition and geochronology as tracers of Paleoproterozoic events
970 at the eastern margin of the East European Craton (Taratash complex, Middle Urals).
971 Lithos, 132-133, 82-97.
972 Smith, H.A. and Giletti, B.J. (1997) Lead diffusion in monazite. Geochimica et Cosmochimica
973 Acta, 61, 1047-1055.
974 Spear, F.S. and Pyle, J.M. (2010) Theoretical modeling of monazite growth in a low-Ca
975 metapelite. Chemical Geology, 273, 111-119.
976 Starynkevitch I. (1922) The chemical formula of monazite and several analyses of Russian
977 monazites. Doklady Akad Nauk SSSR, 31, 28-30.
978 Stepanov, A.S., Hermann, J., Rubatto, D., and Rapp, R.P (2012) Experimental study of
979 monazite/melt partitioning with implications for the REE, Th and U geochemistry of
980 crustal rocks. Chemical Geology, 300-301, 200-220.
981 Sun S-s. and McDonough, W.F. (1989) Chemical and isotopic systematic of ocean basalts:
982 implications for mantle composition and processes. Geological Society of London
983 Special Publications, 42, 313-345.
984 Suzuki, K., Adachi, M., and Kajizuka, I. (1994) Electron microprobe observations of Pb
985 diffusion in metamorphosed detrital monazites. Earth and Planetary Science Letters, 128,
986 391-405.

987 Swain, G.M., Teasdale, H.J., Rutherford, L., and Clark, C. (2005) Age constraints on terrane-
988 scale shear zones in the Gawler Craton, southern Australia. Precambrian Research, 139,
989 164-180.
990 Teufel, S. and Heinrich, W. (1997) Partial resetting of the U-Pb isotope system in monazite
991 through hydrothermal experiments: an SEM and U-Pb isotope study. Chemical Geology,
992 137, 273-281.
993 Tilton, G.R. and Nicolaysen, L.O. (1957) The use of monazite for age determination.
994 Geochimica and Cosmochimica Acta, 11, 28-40.
995 Townsend, K.J., Miller, C.F., D'Andrea, J.L., Ayers, J.C., Harrison, T.M., and Coath, C.D.
996 (2000) Low temperature replacement of monazite in the Ireteba granite, Southern
997 Nevada: Geochronological implications. Chemical Geology, 172, 95-112.
998 Triantafyllidis, S., Pe-Pier, G., MacKay, R., Piper, D.J.W., and Strathdee, G. (2010) Monazite as
999 a provenance indicator for the Lower Cretaceous reservoir sandstones, Scotian Basin.
1000 Geological Survey of Canada Open File, 6732, 452p.
1001 Upadhyay, D. and Pruseth, K.L. (2012) Fluid-induced dissolution breakdown of monazite from
1002 Tso Morari complex, NW Himalayas: evidence for immobility of trace elements.
1003 Contributions to Mineralogy and Petrology, 164, 303-316.
1004 Van Emden, B., Thornber, M.R., Graham, J. and Lincoln, F.J. (1997b) The incorporation of
1005 actinides in monazite and xenotime from placer deposits in western Australia. Canadiam
1006 Mineralogist, 35, 95-104.
1007 Van Emden, B., Thornber, M.R., Graham, J., and Lincoln, F.J. (1997a) Solid solution behaviour
1008 of synthetic monazite and xenotime structure refinement of powder data. Advances in X-
1009 ray Analysis, JCPDS-International Centre for Diffraction Data, 40, 402-412.

1010 Vavra, G. and Schaltegger, U. (1999) Post-granulite facies monazite growth and rejuvenation
1011 during Permian to Lower Jurassic thermal and fluid events in the Ivrea Zone (Southern
1012 Alps). Contributions to Mineralogy and Petrology, 134, 405-414.
1013 Wall, F. and Mariano, A.N. (1996) Rare earth minerals in carbonatites: a discussion centred on
1014 the Kangankunde Carbonatite, Malawi. In A.P. Jones, F. Wall and T.C. Williams, Eds.,
1015 Rare earth minerals: chemistry, origin and ore deposits. Mineralogical Society Series, 7,
1016 193-225, Chapman and Hall, London.
1017 Wan, Y., Li, R., Wilde, S., Liu, D., Chen, Z., Yan, L., Song, T., and Yin, X. (2005) UHP
1018 metamorphism and exhumation of the Dabie Orogen, China: Evidence from SHRIMP
1019 dating of zircon and monazite from a UHP granitic gneiss cobble from the Hefei Basin.
1020 Geochimica et Cosmochimica Acta, 69, 4333-4348.
1021 Wark, D.A. and Miller, C.F. (1993) Accessory mineral behavior during differentiation of a
1022 granite suite: monazite, xenotime and zircon in the Sweetwater Wash pluton,
1023 southeastern California, U.S.A. Chemical Geology, 110, 49-67.
1024 Watson, E.B. and Liang, Y. (1995) A simple model for sector zoning in slowly grown crystals:
1025 Implications for growth rate and lattice diffusion, with emphasis on accessory minerals in
1026 crustal rocks. American Mineralogist, 80, 1179-1187.
1027 Watt, G.R. (1995) High-thorium monazite-(Ce) formed during disequilibrium melting of
1028 metapelites under granulite-facies conditions. Mineralogical Magazine, 59, 735-743.
1029 Wawrzenitz, N., Krohe, N., Rhede, D., and Romer, R.L. (2012) Dating rock deformation with
1030 monazite: The impact of dissolution precipitation creep. Lithos, 134-135, 52-74.
1031 Williams, M.L., Jercinovic, M.J., Harlov, D.E., Budzyń, B., and Hetherington, C.J. (2012)
1032 Resetting monazite ages during fluid-related alteration. Chemical Geology, 283, 218-225.

1033 Williams, M.L., Jercinovic, M.J., and Hetherington, C.J. (2007) Microprobe monazite
1034 geochronology: understanding geologic processes by integrating composition and
1035 chronology. Annual Review of Earth and Planetary Sciences 35, 137-175.
1036 Wing, B.A., Ferry, J.M., and Harrison, T.M. (2003) Prograde destruction and formation of
1037 monazite and allanite during contact and regional metamorphism of pelites: petrology
1038 and geochronology. Contributions to Mineralogy and Petrology 145, 228-250.
1039 Xie, L., Wang, R.C., Wang, D.Z., and Qui, J.S. (2006) A survey of accessory mineral
1040 assemblages in peralkaline and more aluminous A-type granites of the southeast coastal
1041 area of China. Mineralogical Magazine, 70, 709-729.
1042 Yang, P. and Pattison, D. (2006) Genesis of monazite and Y zoning in garnet from the Black
1043 Hills, South Dakota. Lithos, 88, 233- 253.
1044 Yang, P. and Rivers, T. (2002) The origin of Mn and Y annuli in garnet and the thermal
1045 dependence of P in garnet and Y in apatite in calc-pelite and pelite, Gagnon terrane,
1046 western Labrador. Geological Materials Research, 4, 1-35.
1047 Zeh, A. (2006) Calculation of garnet fractionation in metamorphic rocks, with application to a
1048 flat-top, Y-rich garnet population from the Ruhla Crystalline Complex, Central Germany.
1049 Journal of Petrology, 47, 2335-2356.
1050 Zhou, X., Zhao, G., Wei, C., Geng, Y., and Sun, M. (2008) EPMA U-Th-Pb monazite and
1051 SHRIMP U-Pb zircon geochronology of high-pressure pelitic granulites in the Jiaobei
1052 Massif of the North China craton. American Journal of Science, 308, 328-350.
1053 Zhu, X.K. and O'Nions, R.K. (1999a) Zonation of monazite in metamorphic rocks and its
1054 implications for high temperature thermochronology: a case study from the Lewisian
1055 terrain. Earth and Planetary Science Letters, 171, 209-220.

Zhu, X.K. and O'Nions, R.K. (1999b) Monazite chemical composition: some implications for monazite geochronology. Contributions to Mineralogy and Petrology, 137, 351-363.

FIGURE CAPTIONS

Figure 1. Monazite structure after Ni et al. (1995). For other images of the structure, see Huminicki and Hawthorne (2002), Williams et al. (2007), and Clavier et al. (2011).

Figure 2. Plots of ThO_2+UO_2 (wt%) versus (A) Er_2O_3+Yb_2O_3 (wt%) and (B) Ce_2O_3+La_2O_3 (wt%). Data from the granulite facies rocks from Krenn and Finger (2010) and from A-type granites from Xie et al. (2006).

Figure 3. Chondrite-normalized REE patterns for monazite grains from (A) a granulite facies rock (Krenn and Finger 2010), (B) A-type granites (Xie et al. 2006), (C) sedimentary rocks with low ThO_2+UO_2 (<1 wt%) and (D) with high ThO_2+UO_2 (8-17wt%) (Triantafyllidis et al. 2010). The pink area in (C) shows the overlap of the patterns of the high ThO_2+UO_2 grains and the pink area in (D) is the overlap of the patterns of the low ThO_2+UO_2 analyses. REE normalized to chondrite values reported in Sun and McDonough (1989).

Figure 4. Chondrite-normalized REE patterns for coexisting monazite and allanite in garnet-bearing rocks from the Himalayas. Panels are separated by sample number. See Catlos et al. (2001) for sample locations and Catlos et al. (2002) for analytical conditions. REE normalized to chondrite values reported in Sun and McDonough (1989).

Figure 5. (A) Chondrite-normalized REE patterns for garnet-bearing rocks from the Himalayas. See Catlos et al. (2001) for sample locations and Catlos (2000) for compositions. The data include samples with coexisting monazite and allanite (MA27, MA37B, MA33, MA34B, MA86) and samples with allanite only (MA61A, MA78B, MA79). (B) Whole-

rock Ca and Al contents of these samples averaged to Shaw's (1956) average pelite after Wing et al. (2003). We see no correlation between whole rock composition and the presence of these accessory minerals. Samples from Figure 3 are labeled (MA27, MA34B, MA37B). REE normalized to chondrite values reported in Sun and McDonough (1989).

Figure 6. Radiogenic $^{208}Pb^*$ contents of monazite grains from (A) Turkish metagranites (Catlos et al. 2010) and (B) metapelites (Catlos and Cemen 2005).

Figure 7. (A) Crystal structure of Th-poor and (B) Th-rich monazite after Cressey et al. (1999). The structure of the Th-rich monazite grain was generated using the software JCrystalApplet.

TABLES

Table 1. Types of monazite zoning.

Type	Definition	Reference(s)
Sector	Existence of different compositions in different growth sectors of a single crystal, interpreted to be primary zoning	Dowty (1976); Cressey et al. (1999); Williams et al. (2007); Popova and Churin (2010)
Oscillatory	General term for grain brightness that wavers in a regular fashion	Aleinikoff et al. (2000); Crowley et al. (2008); Kohn and Vervoort (2008)
Lamellar	Distinct 1-3μm-sized zones parallel a growth face, interpreted to be growth zoning	DeWolf et al. (1993)
Patchy, spotted, or	Grain consists of regions marked by smaller, irregular regions of different brightness and	Zhu and O'Nions (1999a) Crowley et al. (2008) Gagne et

patchwork-zoned	composition	al. (2009) Faure et al. (2008) Gasser et al. 2012; Vavra and Schaltegger (1999)
Unzoned, weak, faint, poorly defined	Grain shows little to no zoning even when a high degree of contrast is applied	Gagne et al. (2009); Bruguier et al. (2009)
Moderately, slightly zoned or mostly unzoned	Most of the grain consists of homogenous monazite with only a small region showing complex zoning	Harlov and Förster (2002); Aleinikoff et al. (2000)
Concentric	A sub- to euhedral core surrounded by multiple concentric rings, interpreted as growth zoning	Zhu and O'Nions (1999a) Williams et al. (2007); Swain et al. (2005) Bruguier et al. (2009) Ayers et al. (1999) Vavra and Schaltegger (1999)
Simple	Single distinct core surrounded by a single rim	Zhu and O'Nions (1999a) Kusiak et al. (2008) Gagne et al. (2009) Triantafyllidis et al. (2010)
Complex	Single core of variable shape enveloped by two or more circular rims that may be discontinuous	Zhu and O'Nions (1999a) Kusiak et al. (2008) Gagne et al. (2009) Triantafyllidis et al. (2010) Harlov and Förster

		(2002)
Mottled	Region or entire grain that is inclusion-rich; characteristic of monazite dissolution-reprecipitation	Rasmussen and Muhling (2007) Mahan et al. (2010)
Normal	Grain has low Th core and high Th rim	Zhu and O'Nions (1999a)
Reverse	Grain has high Th core and low Th rim	Zhu and O'Nions (1999a)
Sieve-like	Inclusion-rich grain typical of authigenic nodules	Čopjaková et al. (2011)
Extreme Th zoning	Grain contains regions of high Th content compared to the majority of the grain	Williams et al. (2007); Harlov (2011) Gasser et al. 2012
Intergrowth or irregular	Internal microstructure similar to the intergrowth of two different minerals	Zhu and O'Nions (1999a) Foster et al. (2002); Aleinikoff et al. (2006); Ayers et al. (1999) Gasser et al. 2012
Veining or veined	Grain shows differences in composition or brightness near cracks or veins	Ayers et al. (1999) Ayers et al. (2006); Shaw et al. (2001)

1098 **Table 2.** Th^{4+} substitution mechanisms speculated for natural monazite.

Substitution	Reference
$Th^{4+} + Si^{4+} \rightarrow REE^{3+} + P^{5+}$	Burt (1989); Kartashov et al. (2006); Panda et al. (2003)
$Th^{4+} + Ca^{2+} \rightarrow 2REE^{3+}$	Mohr (1984); Bea (1996); Zhu and O'Nions (1999a); Kartashov et al. (2006); Panda et al. (2003)
Coupled $(Th,U)^{4+} + Ca^{2+} \rightarrow 2REE^{3+}$ and $(Th,U)^{4+} + Si^{4+} \rightarrow REE^{3+} + P^{5+}$	Gramacciolii and Segalstad 1978; Van Emden et al. (1997b); Kartashov et al. (2006)
Coupled $(Th,U)^{4+} + Si^{4} \rightarrow REE^{3+} + P^{5+}$ $(Th,U)^{4+} + Ca^{2+} \rightarrow 2REE^{3+}$	Förster (1998); Zhu and O'Nions (1999a); Dawood and El-Naby (2007)
$2(Th,U)^{4+} + Si^{4} \rightarrow Ca^{2+} + 2P^{5+}$ (rare in granites)	Förster (1998)
$(Th^{4+}{}_{1-x} + Ca^{2+}{}_{2+x}) + Si^{4+} \rightarrow REE^{3+} + P^{5+}$	Dana et al. (1951); Semenov (2001); Popova and Churin (2010)
$3(Th,U)^{4+} + \text{vacancy} \rightarrow 4REE^{3+}$	Podor 1994; Clavier et al. 2011

1099

1100

1101

1102

1103

1104

Table 3. Electronic Table of Shannon (1976) Ionic Radii.

Ion	Configuration	Coordination Number	Ionic Radius
Pb^{+2}	$6s^2$	9	1.35
La^{+3}	$4d^{10}$	9	1.216
Ce^{+3}	$6s^1$	9	1.196
Ca^{+2}	$3p^6$	9	1.18
Nd^{+3}	$4f^3$	9	1.163
Gd^{3+}	$4f^7$	9	1.107
Th^{+4}	$6p^6$	9	1.09
Y^{+3}	$4p^6$	9	1.075
Er^{+3}	$4f^{11}$	9	1.062
Yb^{+3}	$4f^{13}$	9	1.042
U^{+4}	$5f^2$	9	1.05
Pb^{+4}	$5d^{10}$	8	0.94

Note: Data downloaded from the Electronic Table of Shannon Ionic Radii, J. David Van Horn (2001).

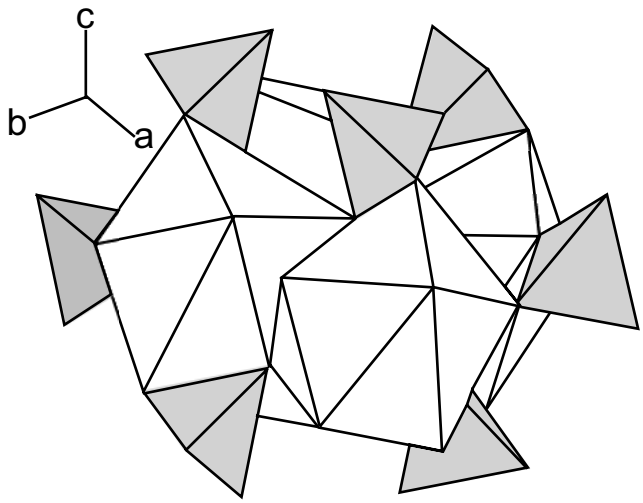

Catlos Figure 1

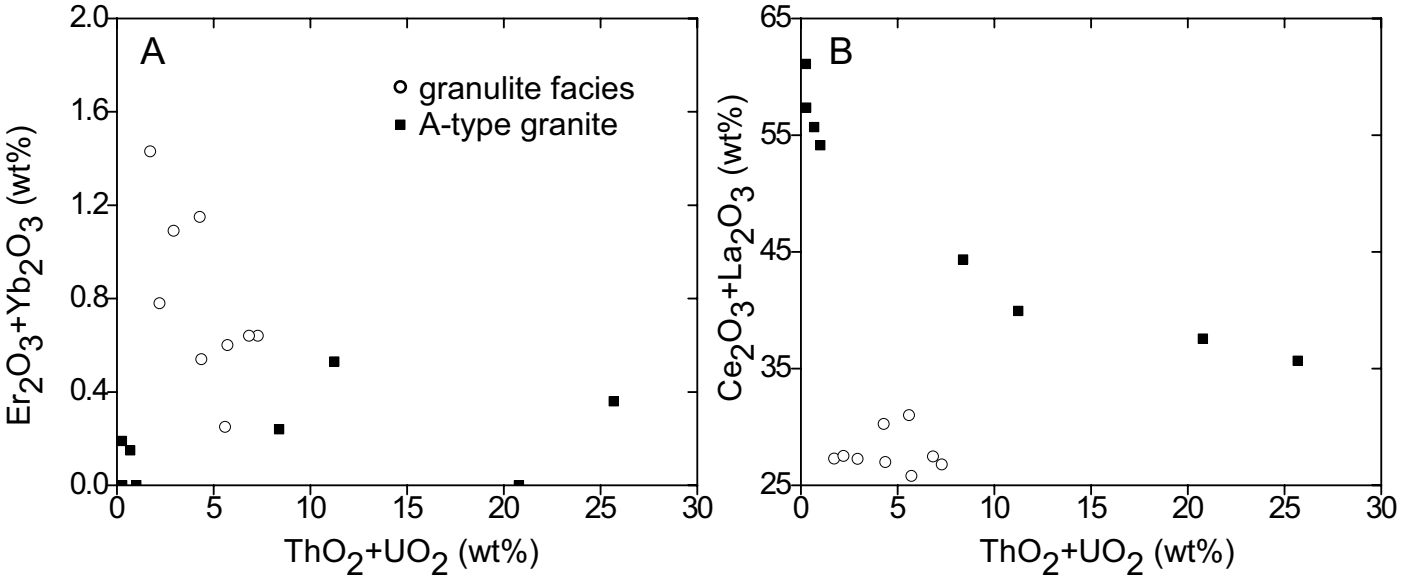

Catlos Figure 2

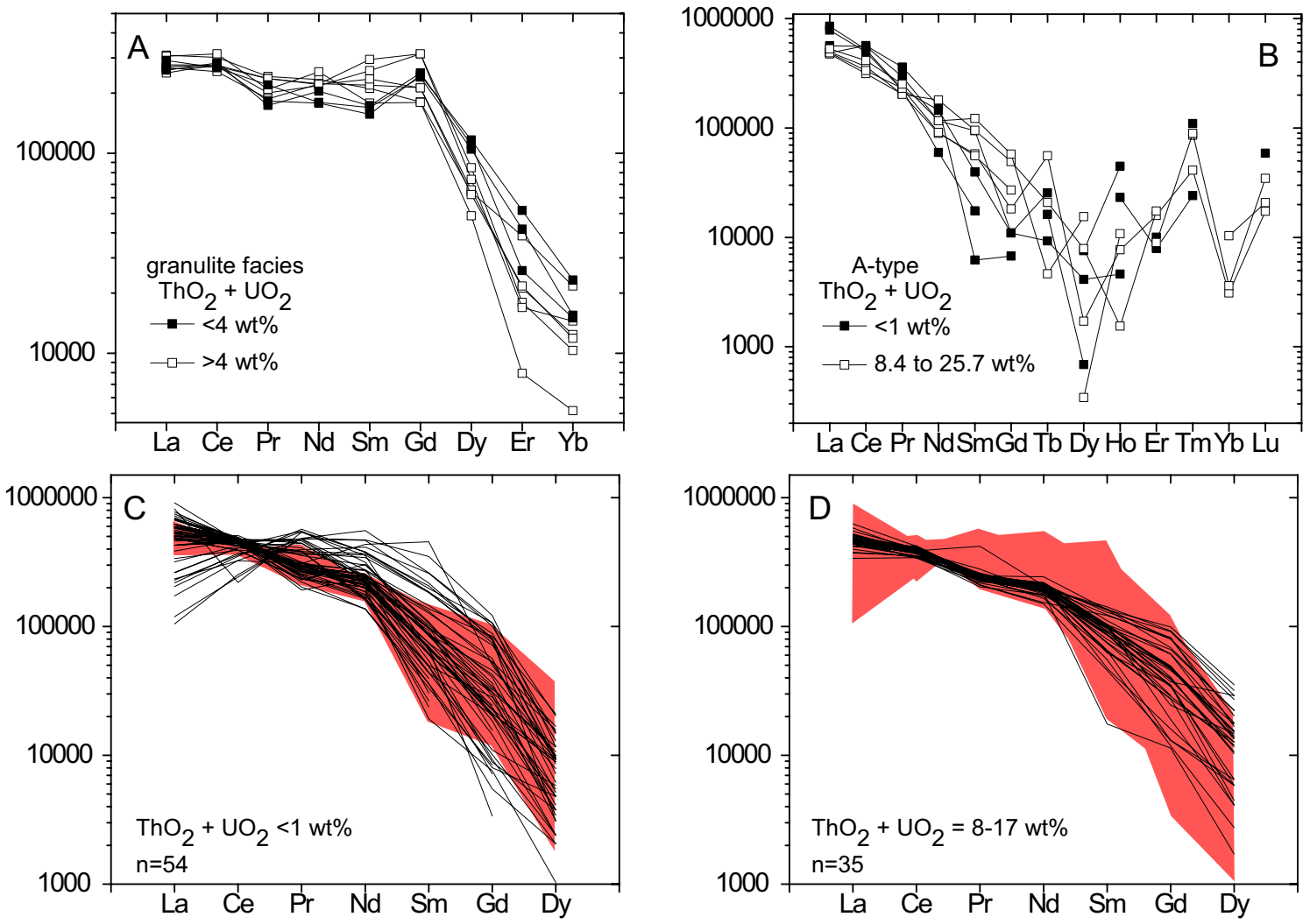

Catlos Figure 3

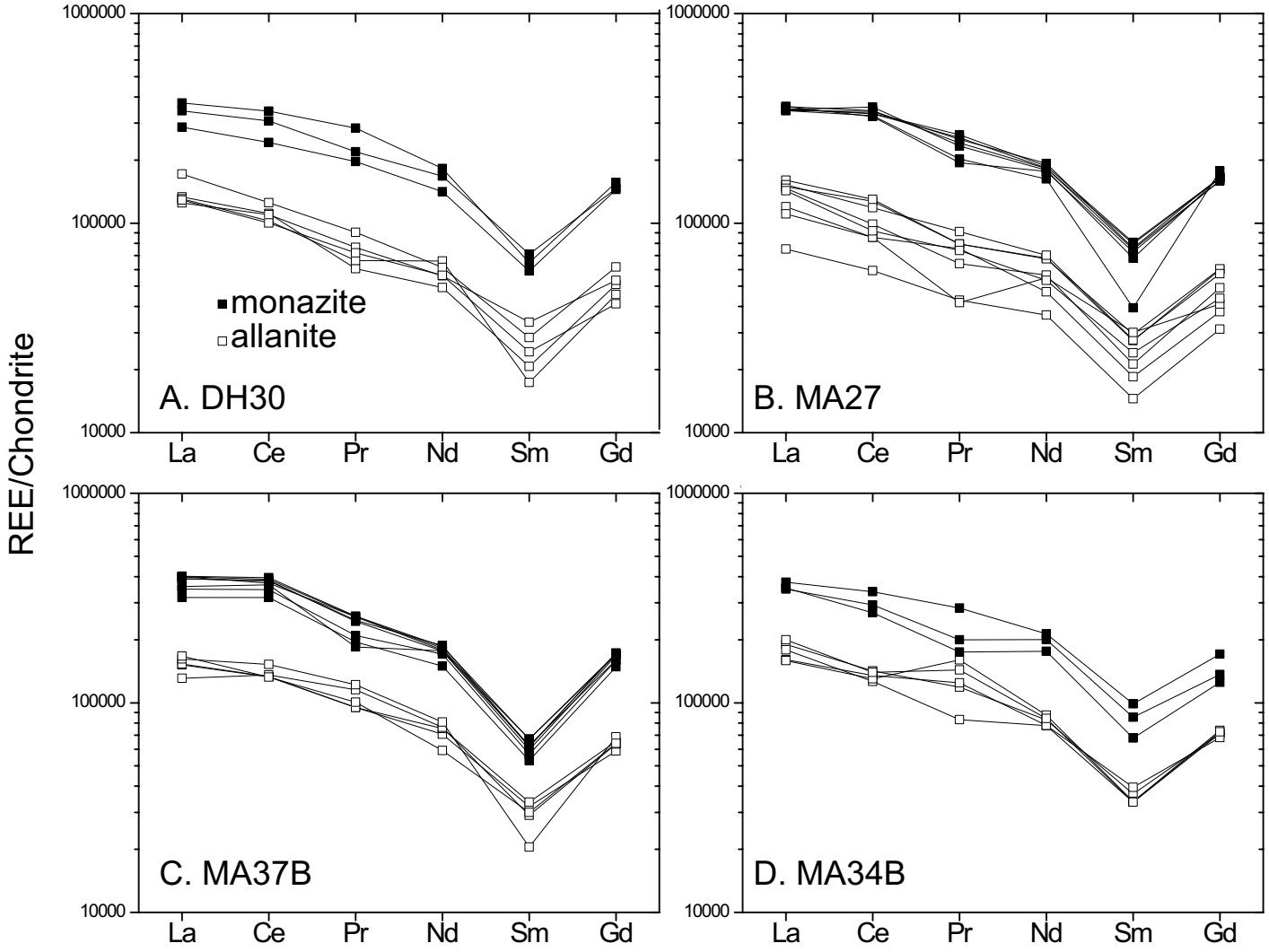

Catlos Figure 4

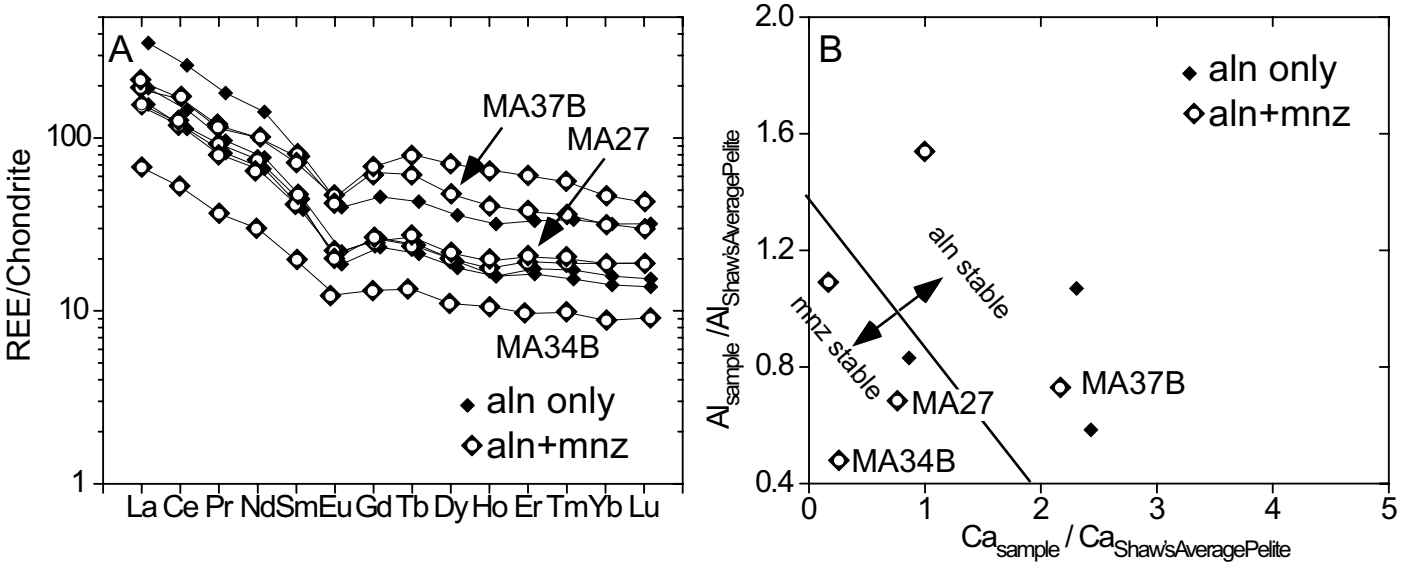

Catlos Figure 5

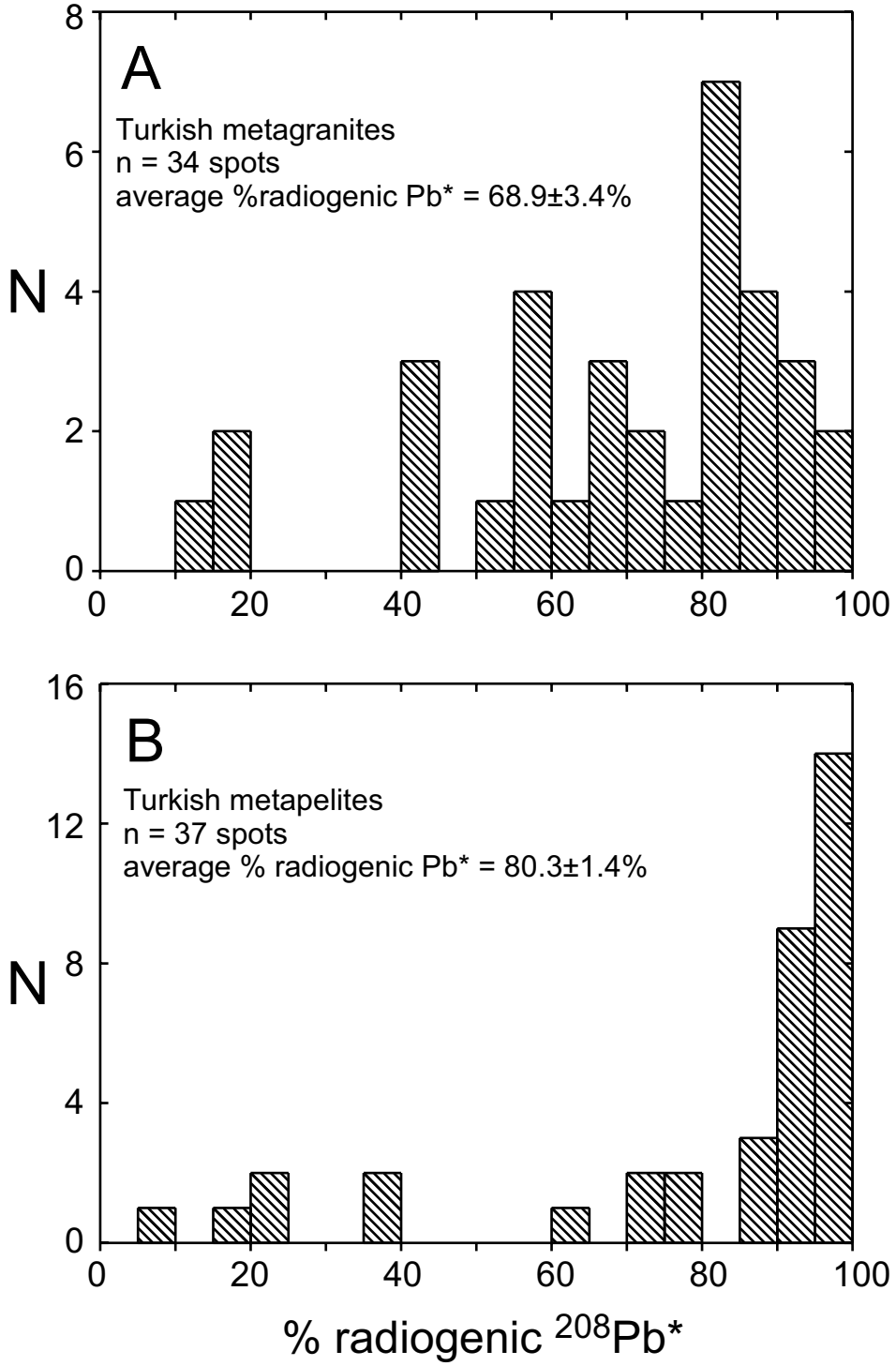

Catlos Figure 6

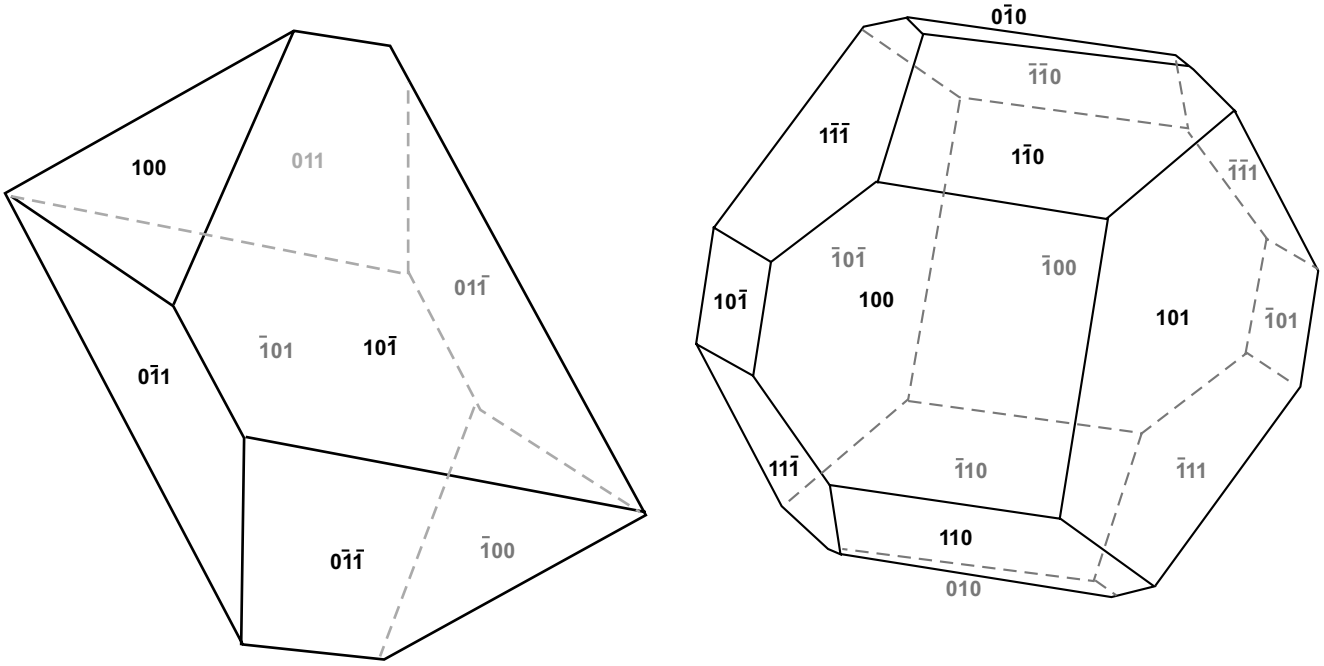

A. Th-poor monazite B. Th-rich monazite

Catlos Figure 7